



The Abdus Salam
International Centre for Theoretical Physics



SMR.1664 - 18

Conference on Single Molecule Magnets and Hybrid Magnetic Nanostructures

27 June - 1 July 2005

Magnetic and Microwave Studies of Single Molecule Magnets

Andrew KENT
Department of Physics
New York University
4 Washington Place
New York, NY 10003
U.S.A.

These are preliminary lecture notes, intended only for distribution to participants



Magnetic and Microwave Studies of Single Molecule Magnets

ANDREW D. KENT
ENRIQUE DEL BARCO

Department of Physics, New York University

In collaboration with:

En-Che Yang, E. Rumberger, and D. N. Hendrickson

Department of Chemistry and Biochemistry, University of California San Diego

N. Chakov and G. Christou

Department of Chemistry, University of Florida

S. Hill

Department of Physics, University of Florida



Outline

I. Introduction

II. QTM in Mn_{12} -acetate

- Experiments with a high field vector superconducting magnet
- QTM probability versus angle of the applied field
- Symmetry of QTM

III. Microwave Spectroscopy and Magnetometry

- SMM Ni_4
- Photon induced transitions between superposition states
- Energy splitting between superposition states
- Decoherence rate (upper bound)
- Longitudinal (energy) relaxation times
 - Spin-phonon relaxation

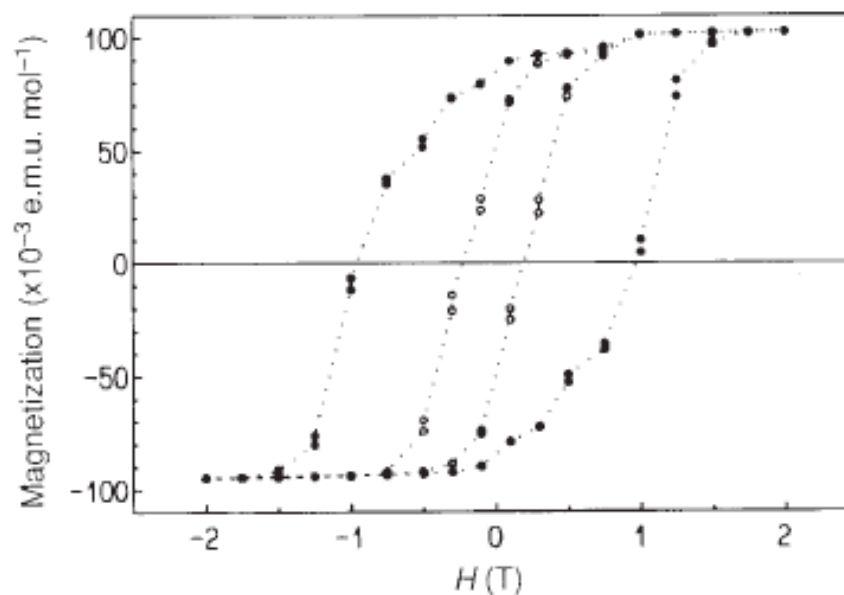
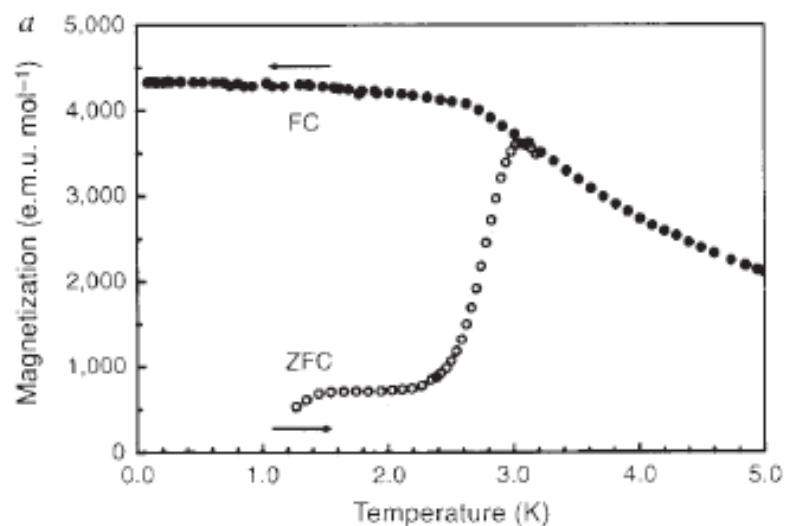
IV. Summary

Magnetic Bistability in a Molecular Magnet

Magnetic bistability in a metal-ion cluster

R. Sessoli*, D. Gatteschi*[†], A. Caneschi*

& M. A. Novak^{‡§} Nature 1993, and Sessoli et al., JACS 1993



Magnetic hysteresis at 2.8 K and below (2.2 K)

S=10 ground state spin

Quantum Tunneling in Single Molecule Magnets

Macroscopic Measurement of Resonant Magnetization Tunneling in High-Spin Molecules

Jonathan R. Friedman and M. P. Sarachik

Department of Physics, The City College of the City University of New York, New York, New York 10031

J. Tejada

Facultat de Física, Universitat de Barcelona, 08028 Barcelona, Spain

R. Ziolo

Wilson Center for Research and Technology, Xerox Corporation, Webster, New York 14580

(Received 1 November 1995)

We report the observation of steps at regular intervals of magnetic field in the hysteresis loop of a macroscopic sample of oriented $\text{Mn}_{12}\text{O}_{12}(\text{CH}_3\text{COO})_{16}(\text{H}_2\text{O})_4$ crystals. The magnetic relaxation rate increases substantially when the field is tuned to a step. We propose that these effects are manifestations of thermally assisted, field-tuned resonant tunneling between quantum spin states, and attribute the observation of quantum-mechanical phenomena on a macroscopic scale to tunneling in a large (Avogadro's) number of magnetically identical molecules. [S0031-9007(96)00131-7]

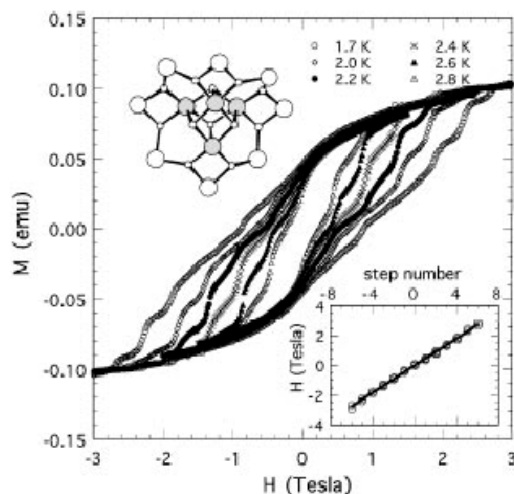


FIG. 1. Magnetization of Mn_{12} as a function of magnetic field at six different temperatures, as shown (field sweep rate of 67 mT/min). The inset shows the fields at which steps occur

Single crystal studies of Mn_{12} : L. Thomas, et al. *Nature* 383, 145 (1996)
Susceptibility studies: J.M. Hernandez, et al. *EPL* 35, 301 (1996)

First SMM: Mn₁₂-acetate



Magnetic Core

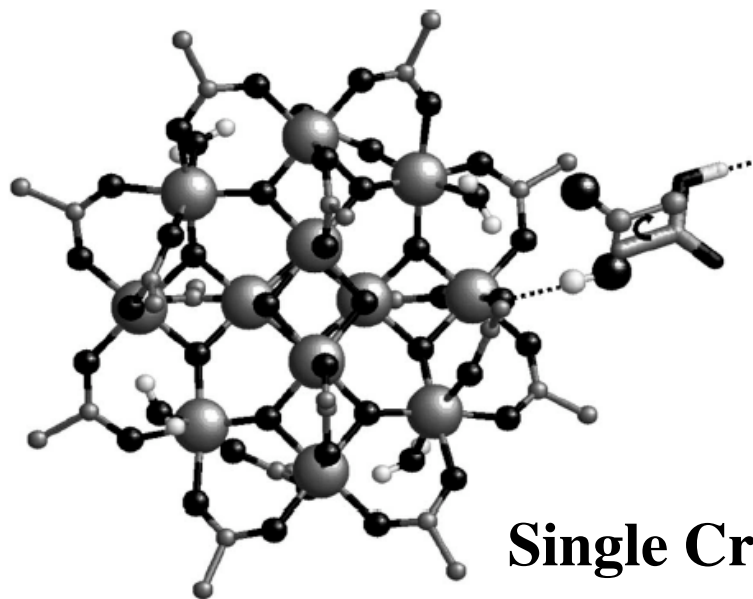
8 Mn³⁺ S=2
4 Mn⁴⁺ S=3/2

Competing AFM
Interactions

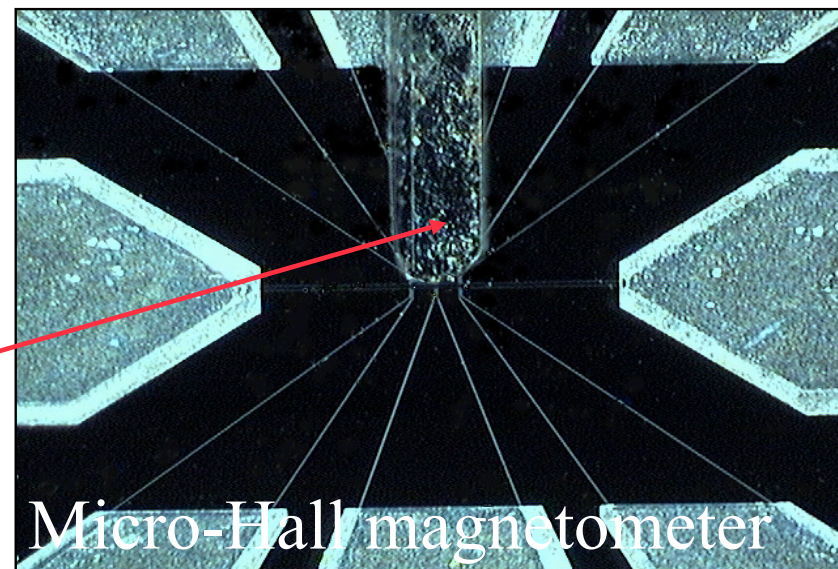
Ground state
S=10

Organic Environment

2 acetic acid molecules
4 water molecules



Single Crystal



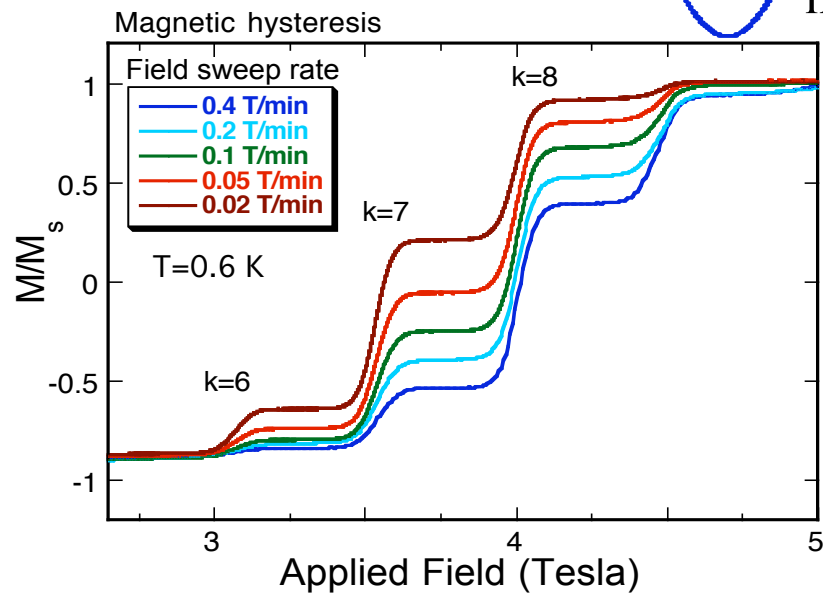
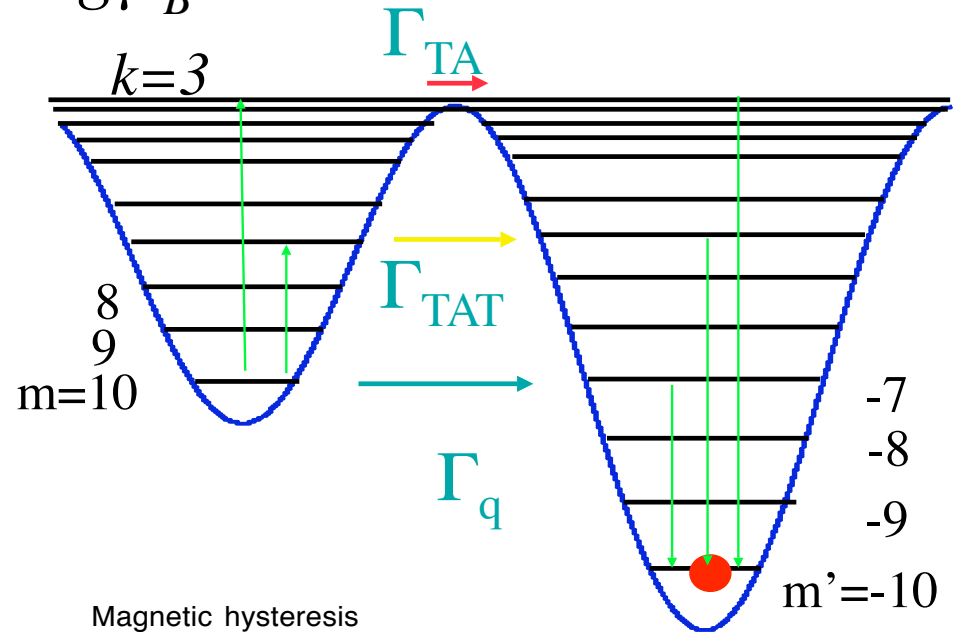
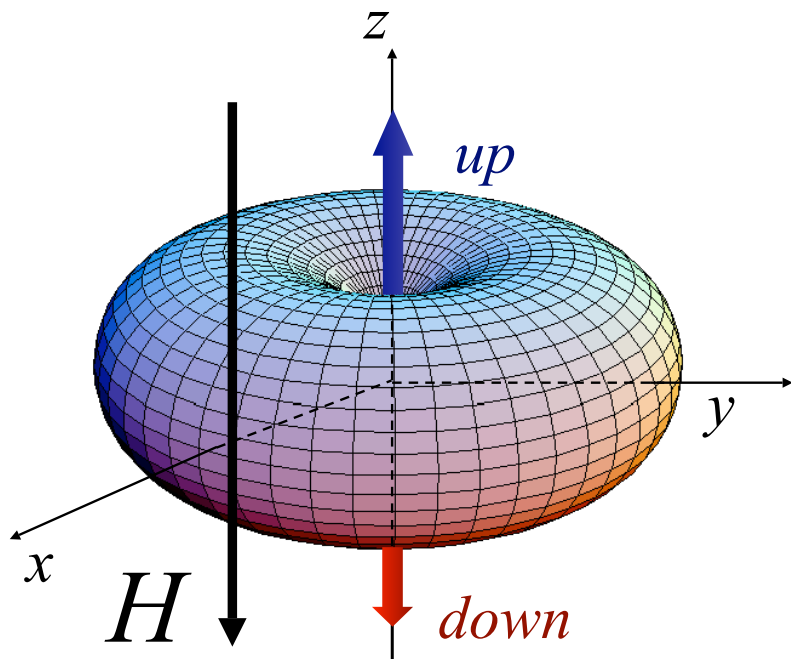
Micro-Hall magnetometer

- S₄ site symmetry
- Tetragonal lattice a=1.7 nm, b=1.2 nm
- Strong uniaxial magnetic anisotropy (~60 K)
- Weak intermolecular interactions (~0.1 K)

Quantum Tunneling of Magnetization

Spin Hamiltonian $H = -DS_z^2 - g\mu_B \vec{S} \cdot \vec{H}$

$H_k = kD/g\mu_B$ (resonances) $k = m + m'$
 $\approx k0.44T$



Questions

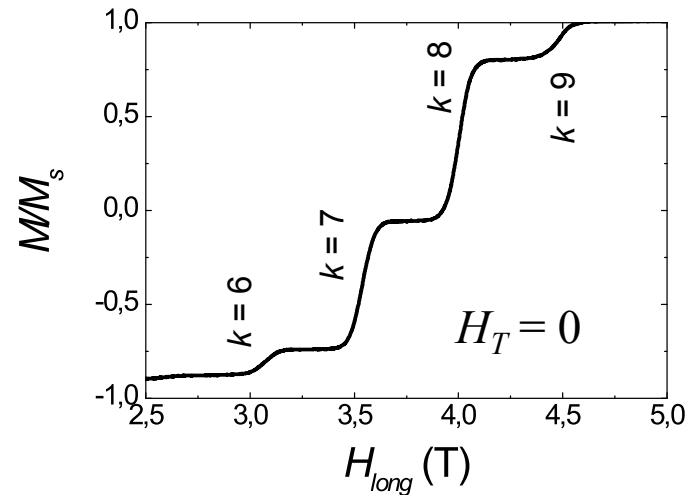
- **What interactions break the axial symmetry and produce QTM?**
 - Magnetic relaxation does not reflect the site symmetry of the molecule
- **Non-exponential relaxation of the magnetization**
 - Broad distribution of relaxation rates (on a logarithmic scale) and thus a broad distribution of tunnel splittings

K. Mertes et al. PRL 2001

Absence of Tunneling Selection Rules

$$H = -DS_z^2 - g\mu_B S_z H_z - g\mu_B S_x H_x$$

0

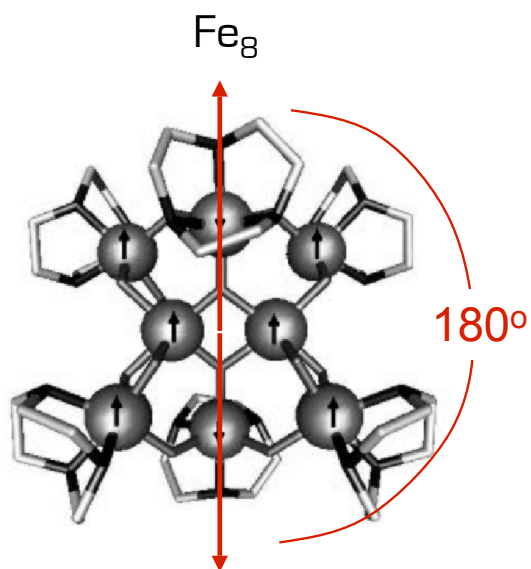


Dipolar and hyperfine fields cannot explain the observed tunneling rates

Absence of Tunneling Selection Rules

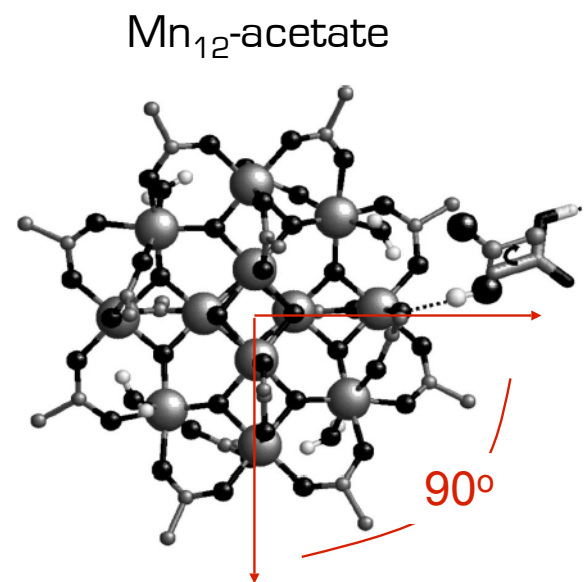
$$H = -DS_z^2 - g\mu_B S_z H_z + H_A$$

Form of H_A determined by the symmetry of the molecules



C₂-site symmetry (rhombic)

$$H_A = E(S_x^2 - S_y^2)$$



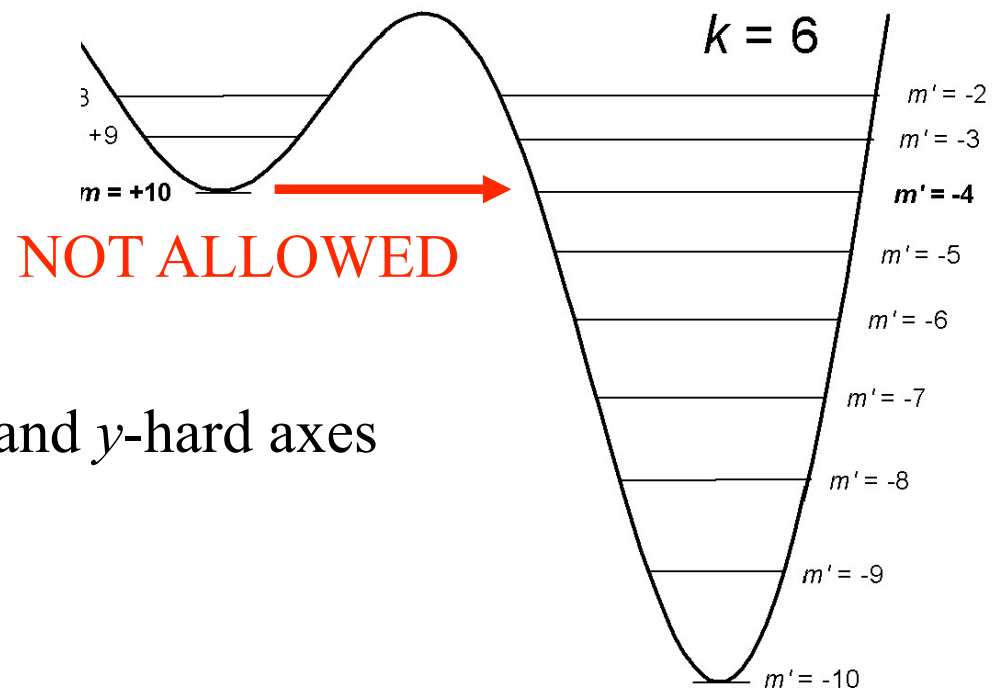
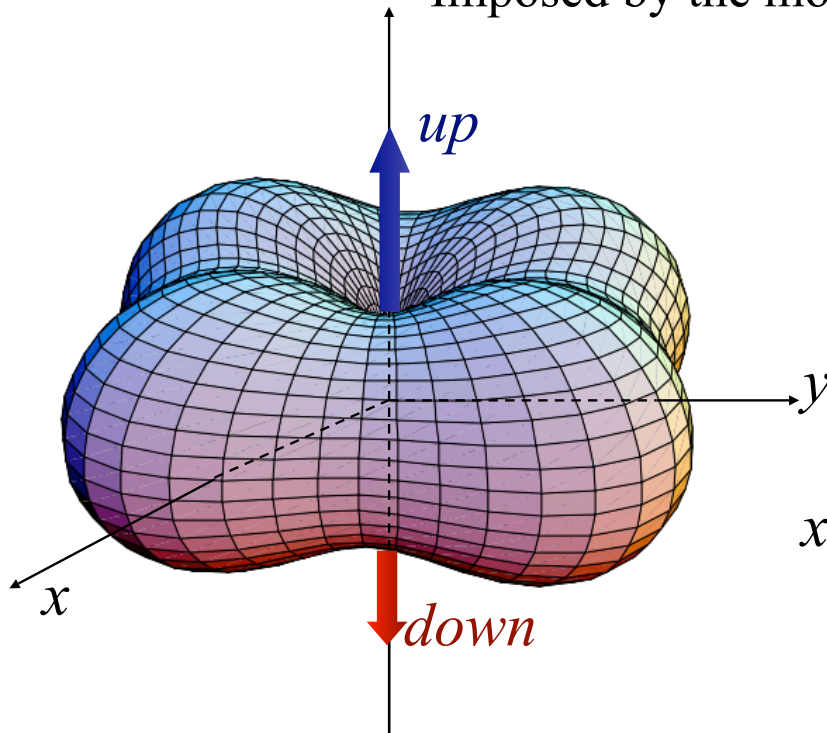
S₄-site symmetry (tetragonal)

$$H_A = C(S_+^4 + S_-^4)$$

QTM and Molecule Symmetry

$$H = -DS_z^2 - BS_z^4 + C(S_+^4 + S_-^4) - g\mu_B \vec{S} \cdot \vec{H}$$

Fourth order transverse anisotropy
Imposed by the molecule S_4 site symmetry



x - and y -hard axes

Fourth order anisotropy only allows transition for $k = 4n$, with $n = \text{integer}$

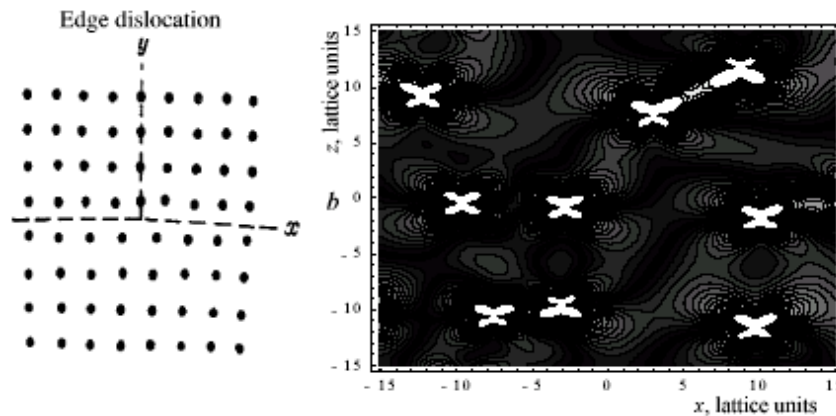
Models of QTM in Mn₁₂-acetate

Disorder lowers the symmetry of the molecules

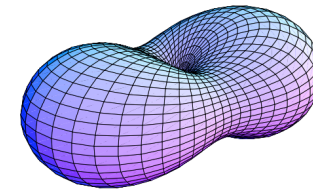
- Absence of tunneling selection rules
- Non-exponential relaxation of the magnetization

1) Dislocation model

Line dislocations generate a broad distribution of second order anisotropy



$$E(S_x^2 - S_y^2)$$



Most probable value
 $E = 0$

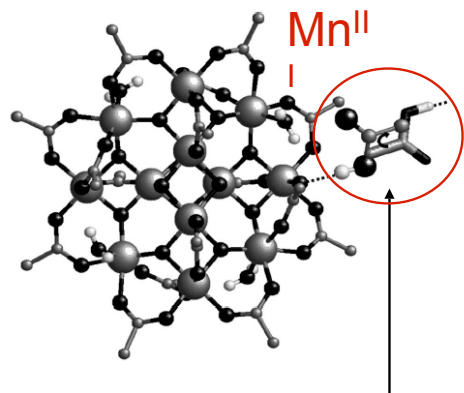
Log-normal Δ distribution

E. M. Chudnovsky and D. A. Garanin,
Phys. Rev. Lett. **87**, 187203 (2001)

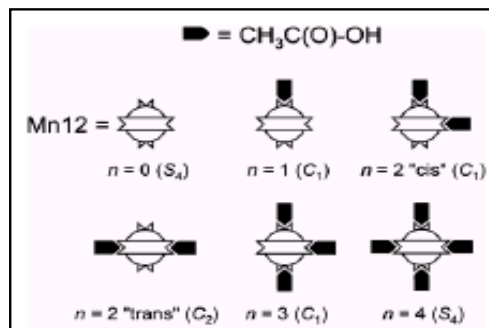
Solvent Disorder Model

Disorder in the solvent molecules generates a discrete set of isomers with second order anisotropy

A. Cornia *et al.*, *Phys. Rev. Lett.* **89**, 257201 (2002)

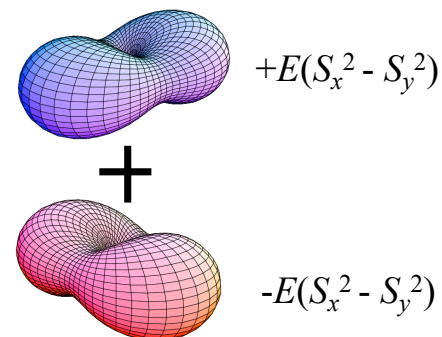


average of 2 CH₃COOH molecules per Mn₁₂
with 4 possible positions



$$\pm E(S_x^2 - S_y^2)$$

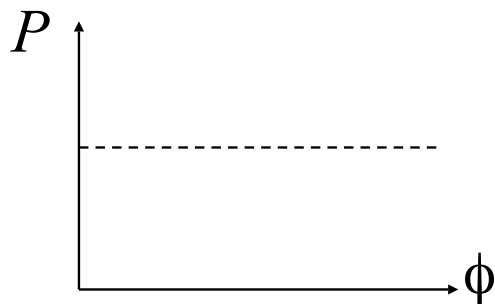
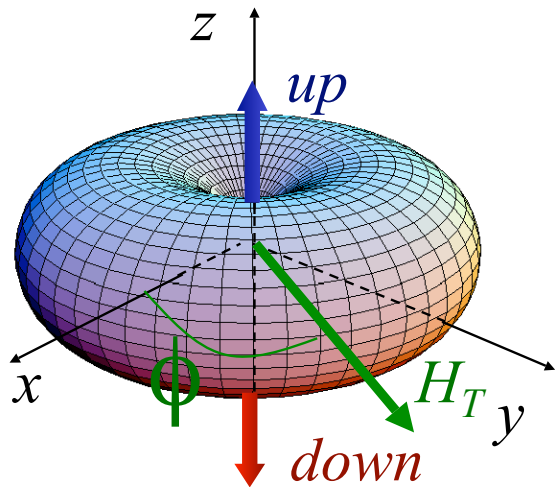
- Most probable $E \neq 0$
- Equal populations of:



Transverse Magnetic Interactions and QTM Symmetry

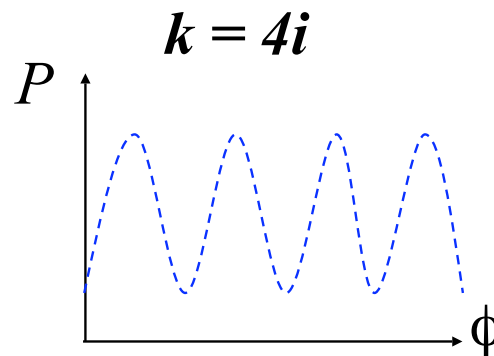
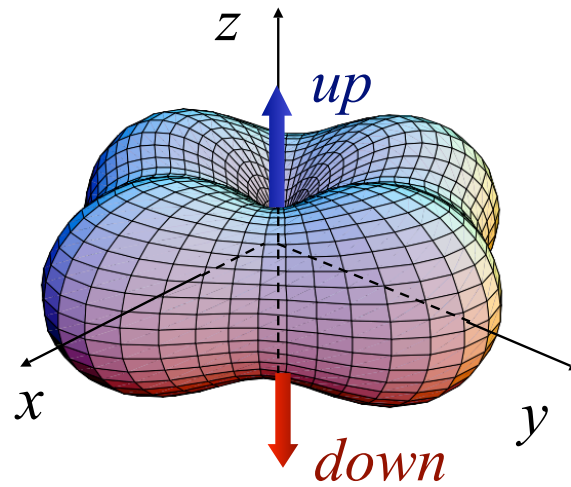
Axial

$$-DS_z^2$$



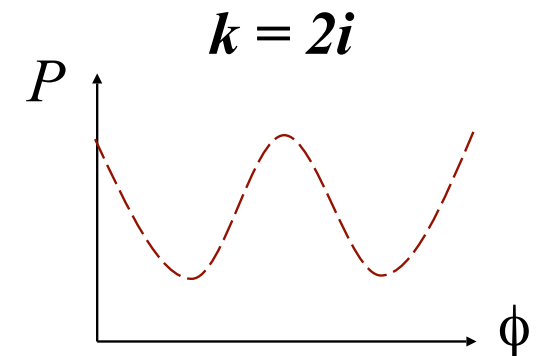
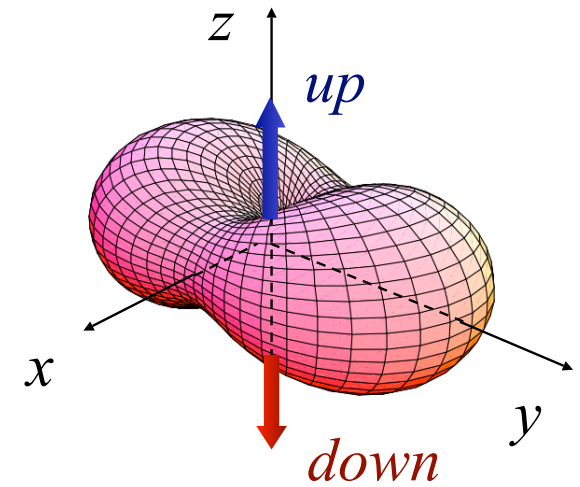
Tetragonal

$$-C(S_+^4 + S_-^4)$$



Orthorhombic

$$-E(S_x^2 - S_y^2)$$

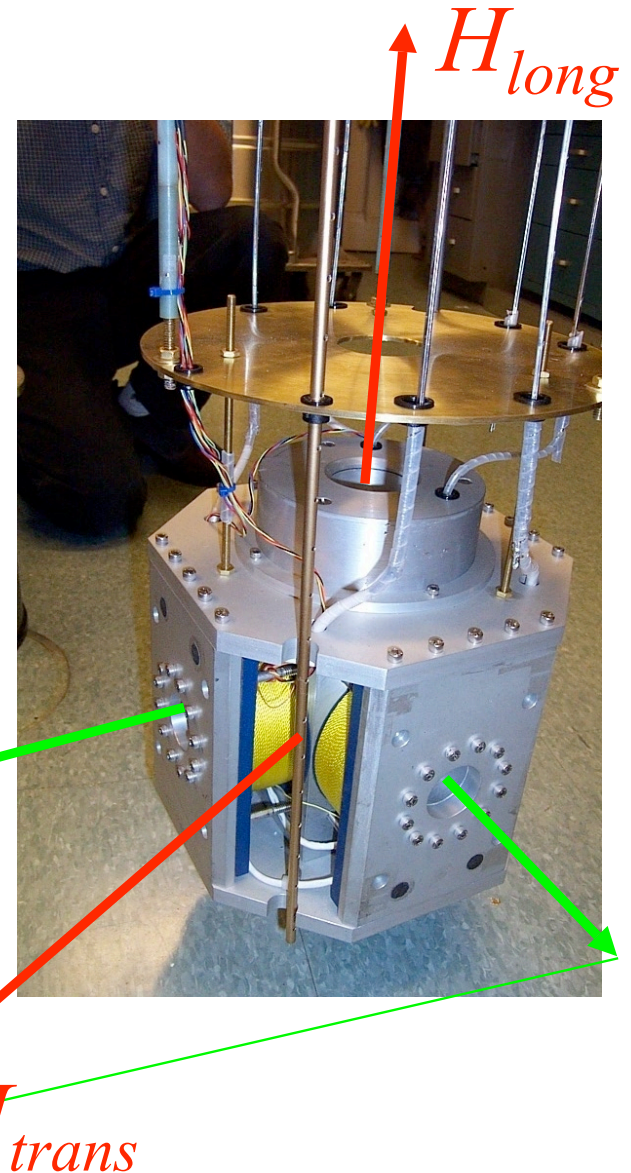
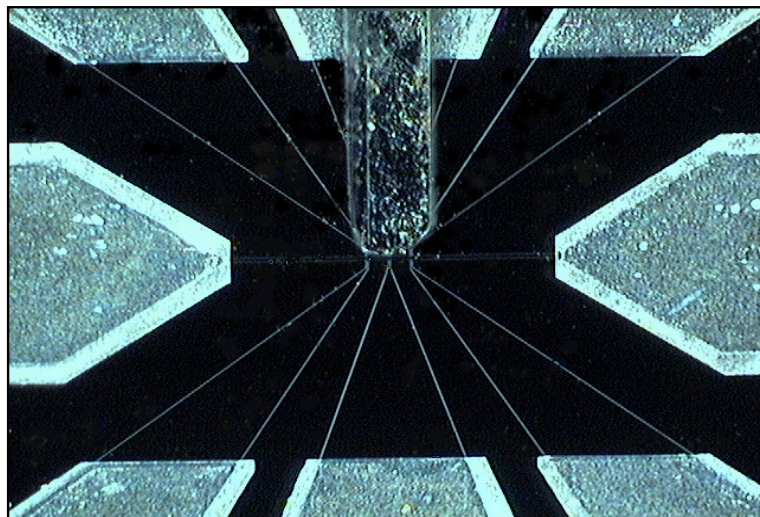




Experiments: Superconducting Vector Magnet

Measure magnetic response to a transverse “probe” field to determine the fundamental symmetry breaking interactions at the origin of MQT

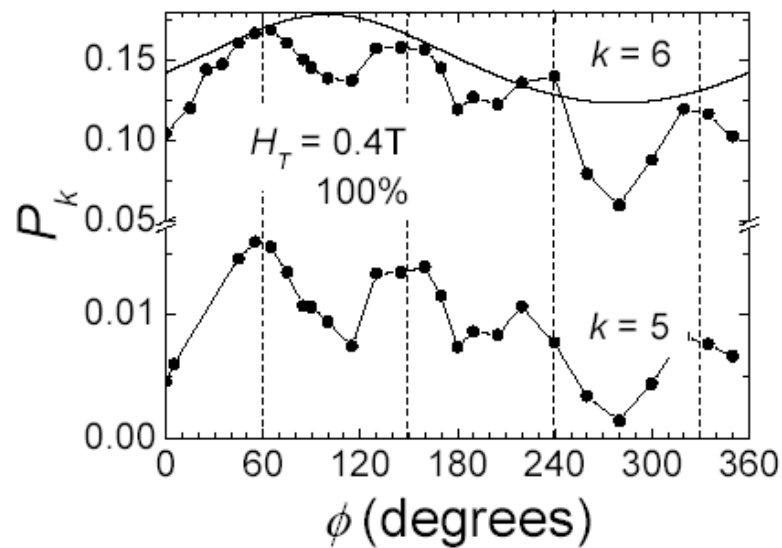
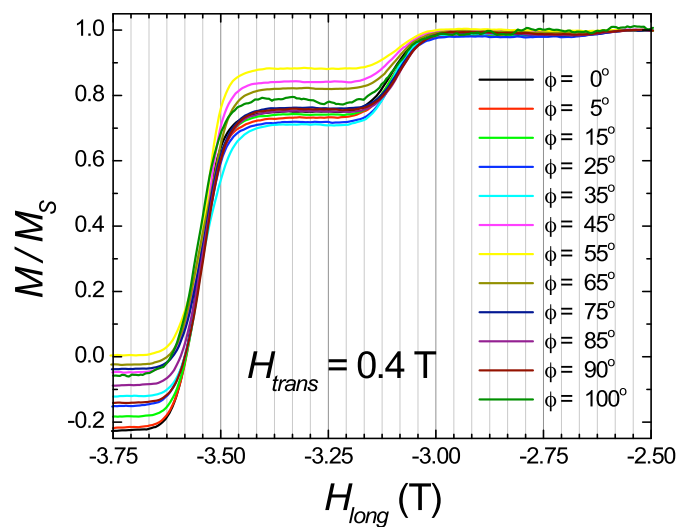
Magnetic measurements



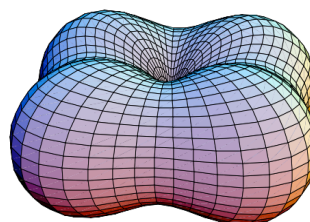
QTM relaxation with transverse fields

Initial magnetization = saturation magnetization

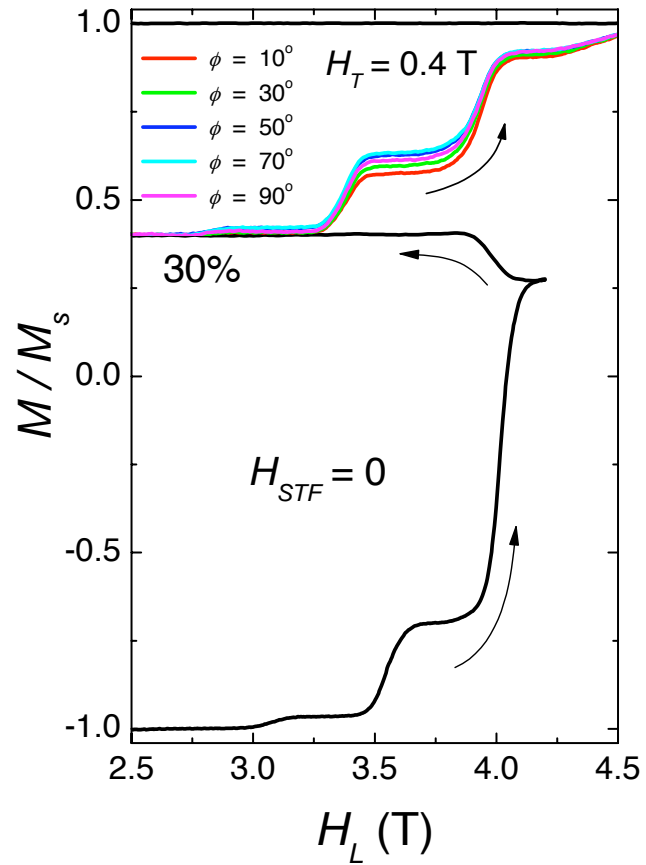
[All the molecules contribute to the relaxation]



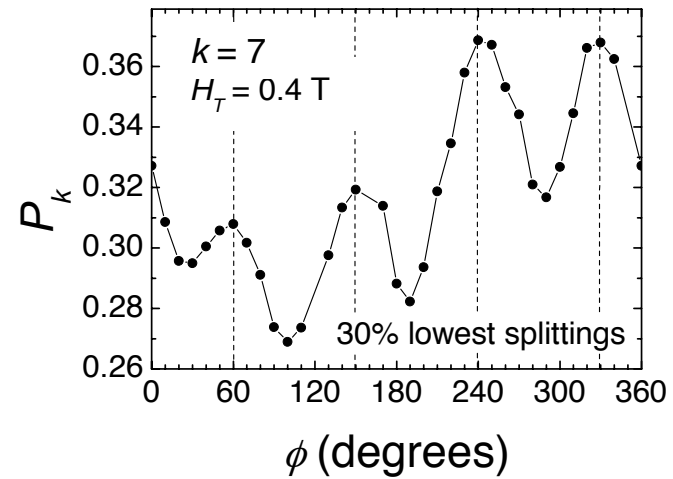
The results show fourfold symmetry



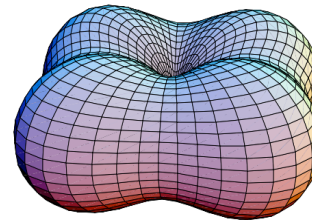
QTM relaxation with transverse fields



Smallest tunnel splittings



Also shows fourfold symmetry

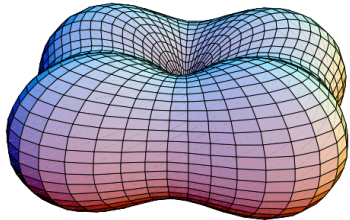


Magnetic relaxation with transverse fields

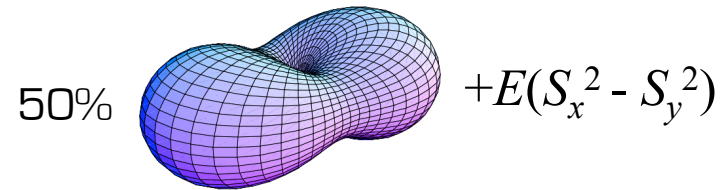
How to distinguish between... ?

fourth order anisotropy

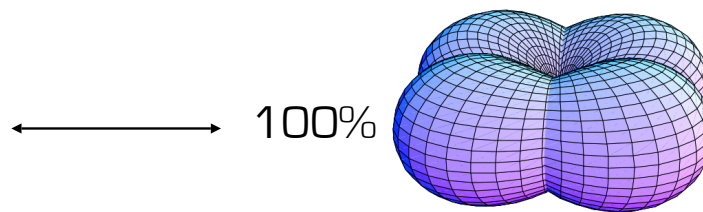
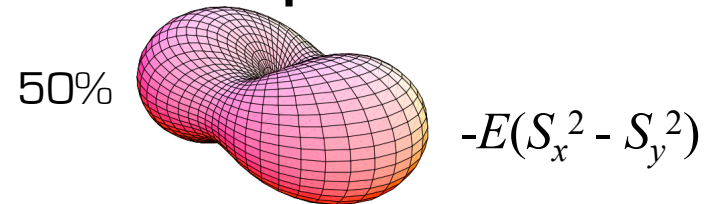
$$C(S_+^4 + S_-^4)$$



Equal populations of molecules
with opposite signs of E

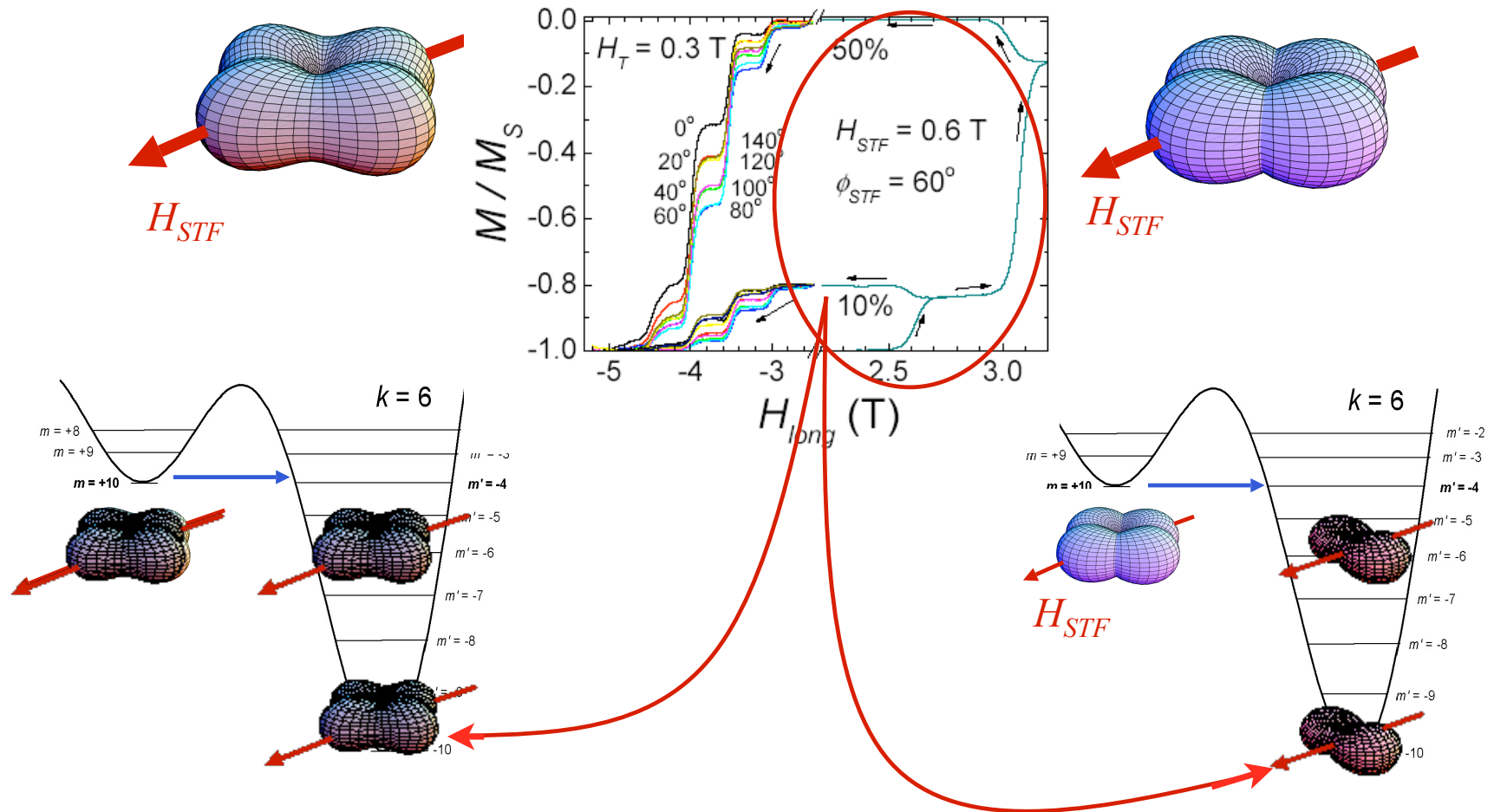


+



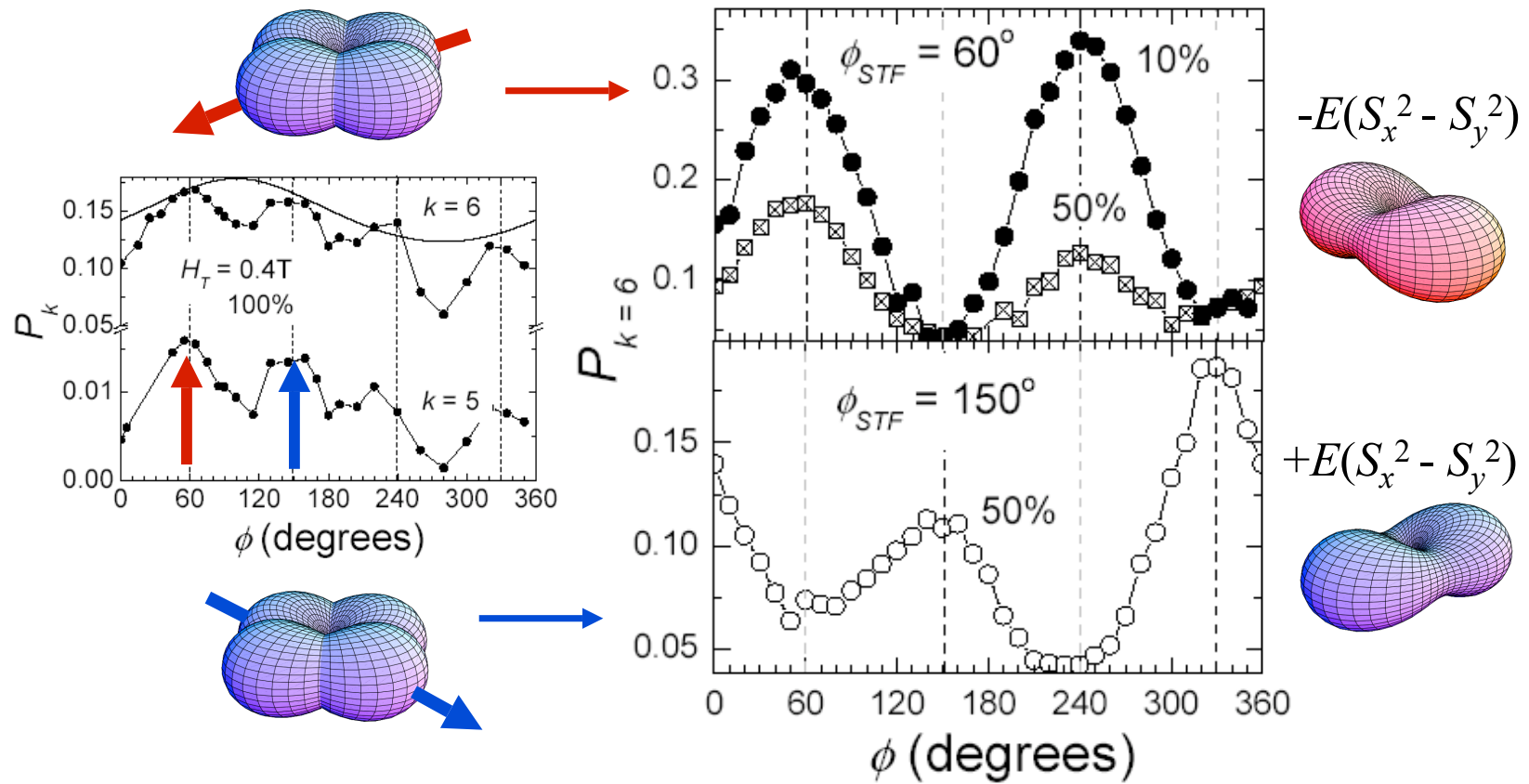
QTM relaxation in the presence of transverse field

Solution: Selection with transverse field, H_{STF}



Magnetic relaxation with transverse fields

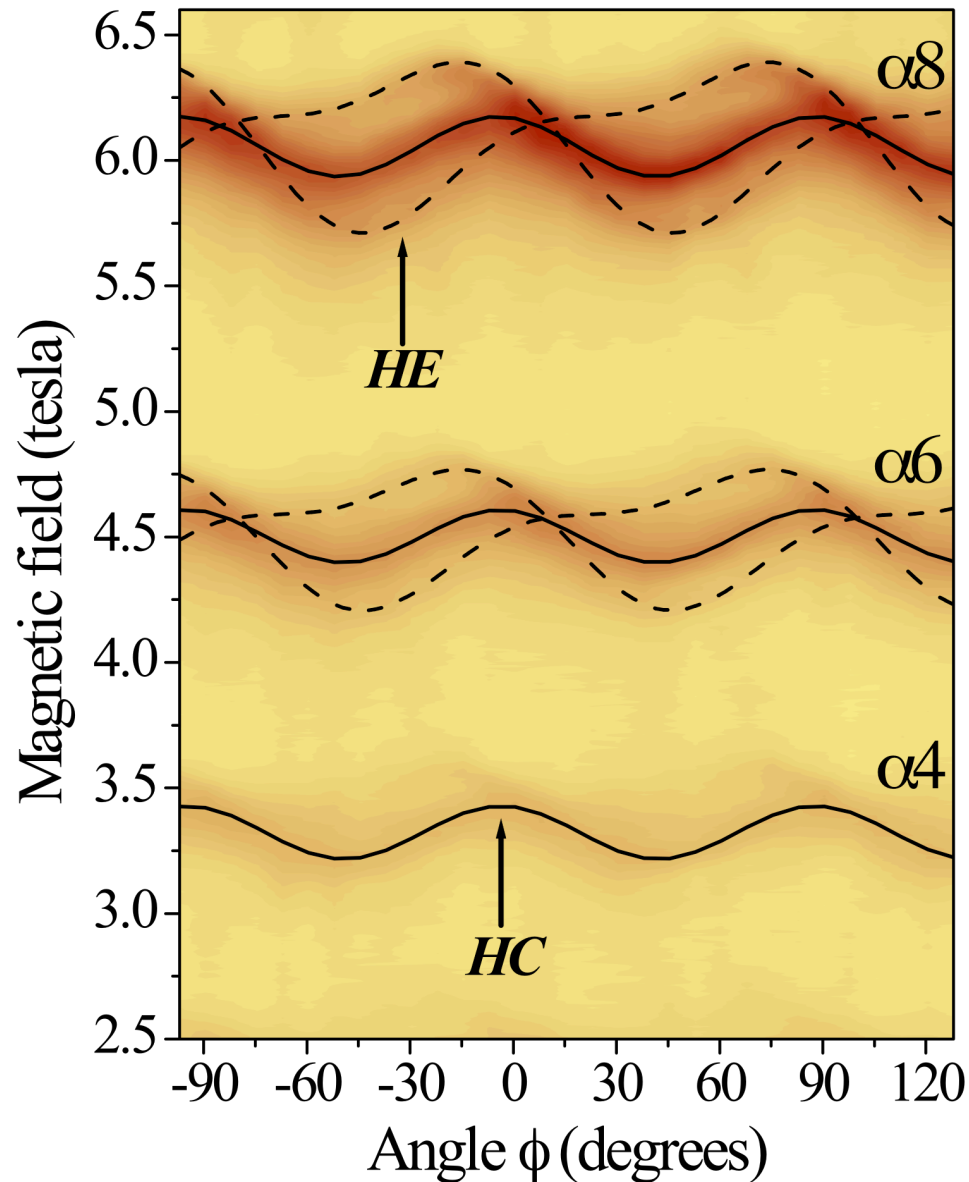
Results:



E. del Barco et al., Phys. Rev. Lett (2003)

Determination of transverse crystal-field interactions in d-Mn₁₂-Ac

Identical to h-Mn₁₂-Ac



- Two-fold line shifts associated with the high- and low-field shoulders due to a quadratic transverse interaction in H_T

del Barco et al., arXiv/cond-mat/0404390

$$E \left(\hat{S}_{x'}^2 - \hat{S}_{y'}^2 \right)$$

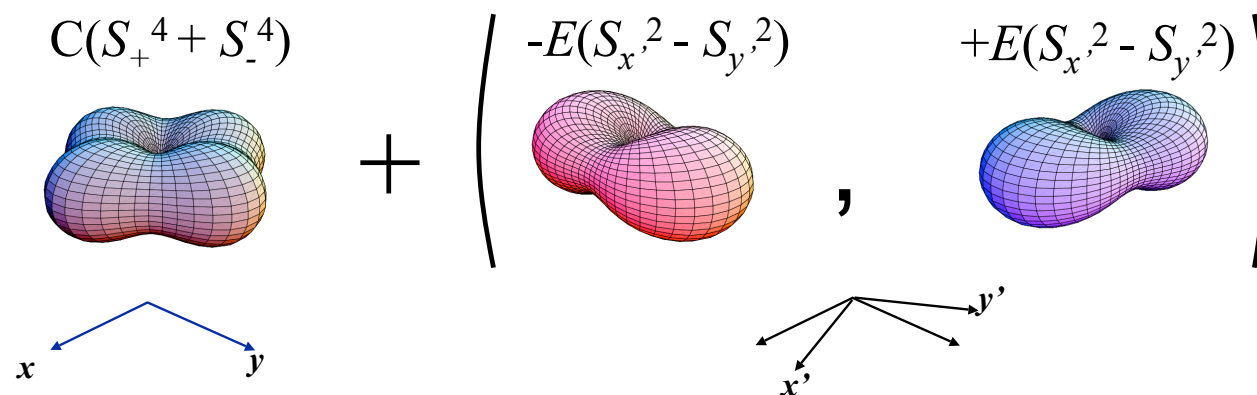
$$E = 20 \text{ mK}$$

Incompatible with the crystallographic symmetry!

HC and HE incommensurate!

Symmetry of QTM

Interpretation of results:



In agreement with solvent disorder model of Cornia et al.

Magnetometry and high frequency EPR studies have come to the conclusion that second and fourth order transverse anisotropies compete: S. Hill, et al. PRL 2003, del Barco et al. cond-mat/0404390 [and to appear in JLTP]

They produce comparable level splittings!

$$\Delta_E \sim D(E/2D)^{(m'-m)/2}$$

$$\Delta_C \sim D(C/2D)^{(m'-m)/4}$$

$$E^2 \sim DC$$

$$E \sim 10^{-2}K, C \sim 10^{-5}K, D \sim 1K$$

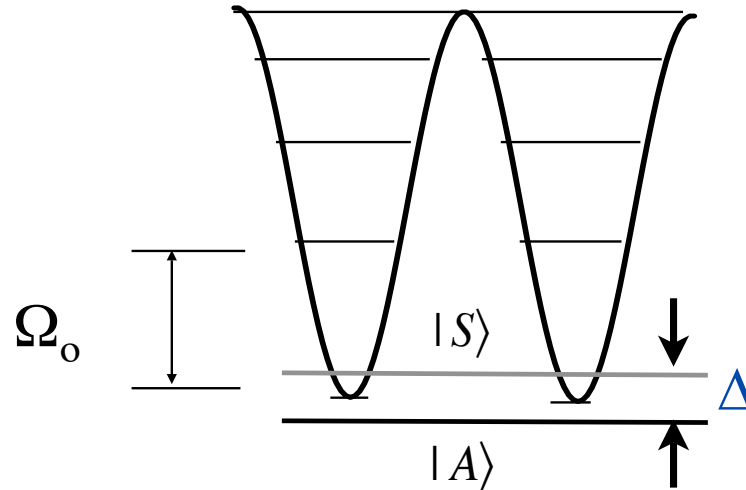
$$\longrightarrow \Delta_E \sim \Delta_C \quad \text{Independent of } m \text{ and } m'!!$$

Summary–Mn₁₂

- Observation of two-fold symmetry in Mn₁₂-acetate:
lower than that of the (average) site symmetry of the molecule
In agreement with the solvent disorder model of Cornia et al.
- Incommensurate 2nd (“E”) and 4th (“C”) order transverse anisotropies.
- Observation of usual Berry phase phenomena in Mn₁₂-acetate
associated with disorder induced + intrinsic transverse anisotropies
- Tilts of the easy axes of the molecules
 - a) Explains the observation of MQT at odd-resonances in this SMM
 - b) Recently observed in Mn₁₂-acetate with EPR spectroscopy
- MQT is very sensitive to local chemical micro-environments:
Implications for molecules on surfaces

Spin Dynamics in Single Molecule Magnets

- **Decoherence**



- **Limit** $\Omega_0 \gg \Delta \gg kT, E_0$

First condition: consider just 2 lowest energy states

Second condition: insures dephasing by phonons and nuclear spins is small
 E_0 typical energy width of nuclear spin multiplet

- **Predictions** (Stamp) for dephasing rate due to nuclear spins in an applied field

$$\Gamma_\varphi = \frac{\pi}{Q} \approx \left(\frac{E_0}{\Delta} \right)^2$$

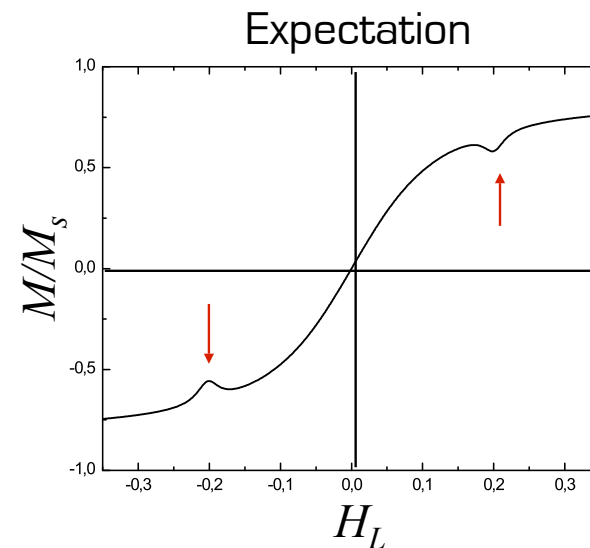
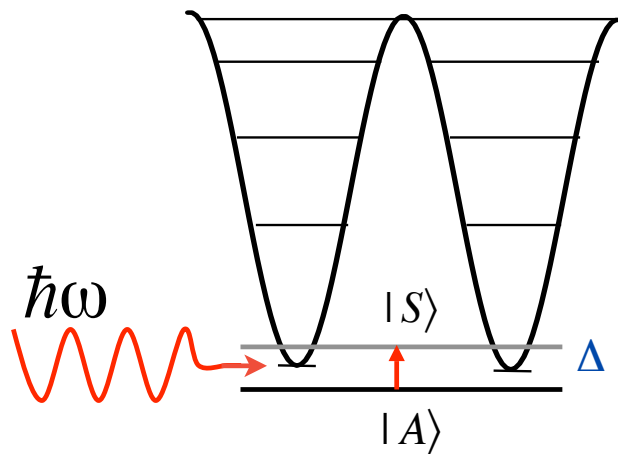
(Chudnovsky) spin-phonon interaction: universal lower bound on decoherence

$$\tau_1^{-1} = \Gamma_1 = \frac{S^2 \Delta^2 \omega^3}{12\pi \hbar^2 \rho c_t^5} \coth\left(\frac{\hbar\omega}{2kT}\right)$$

Experiment

Study: Magnetization Dynamics Induced by Microwaves (cw and pulsed)

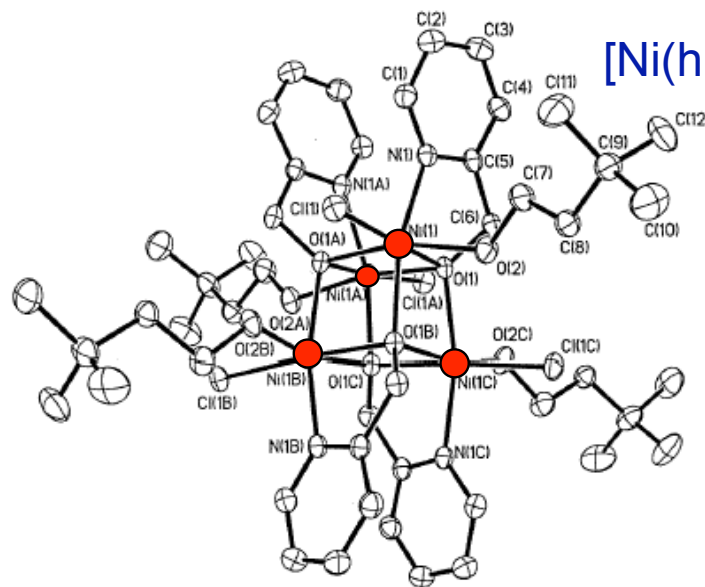
- Photon induced transition between superposition states combined with magnetization measurements



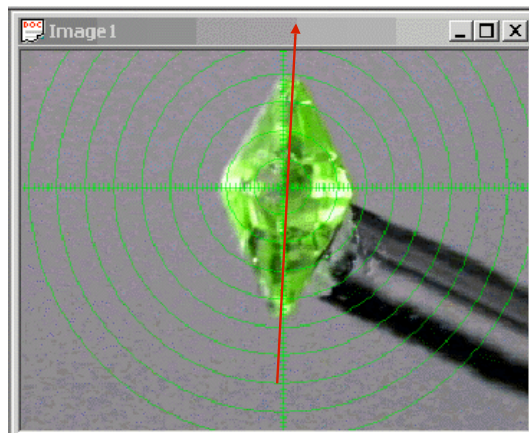
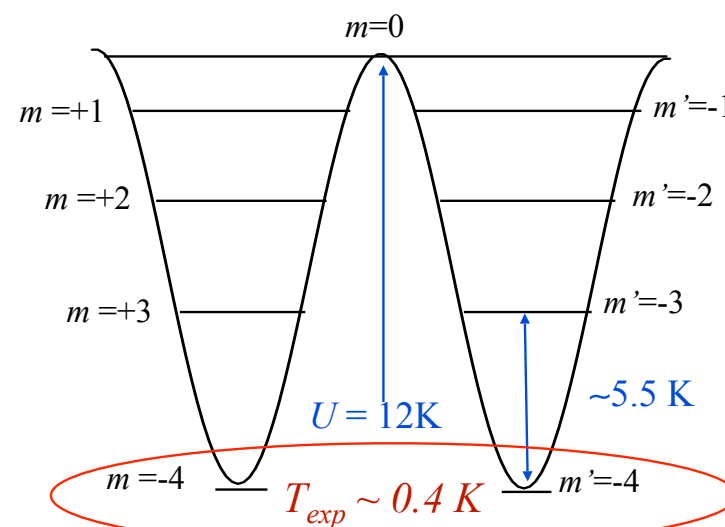
- Monitor spin-state populations while performing microwave spectroscopy
- Pulsed and CW microwave fields
- High magnetic sensitivity: $\sim 10^5$ spins/Hz^{1/2}
- High magnetic fields
- Time resolved magnetic measurements (\sim GHz)

Description of SMM Ni₄

$$H = -DS_z^2 + C(S_+^4 + S_-^4) - g\mu_B S_z H_z - g\mu_B S_x H_x$$



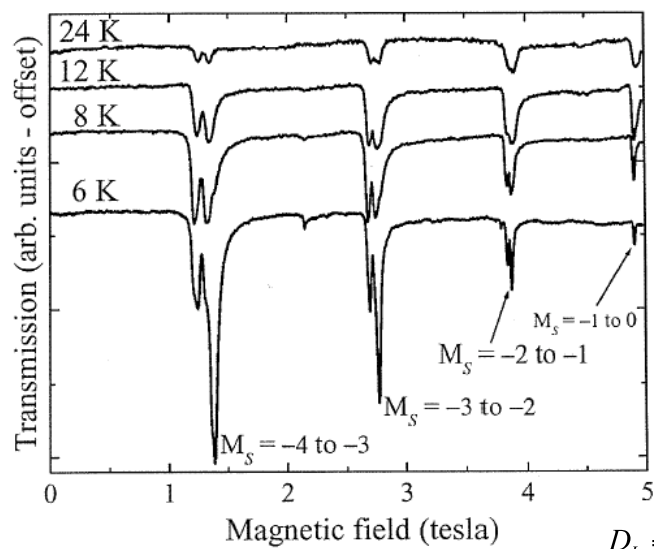
$$S = 4$$



Description of SMM Ni₄

High frequency EPR: *Stephen Hill, UF - Gainesville, FL*

$$H = -DS_z^2 + C(S_+^4 + S_-^4) - g\mu_B S_z H_z - g\mu_B S_x H_x$$



$$D_L = -0.600 \text{ cm}^{-1}$$

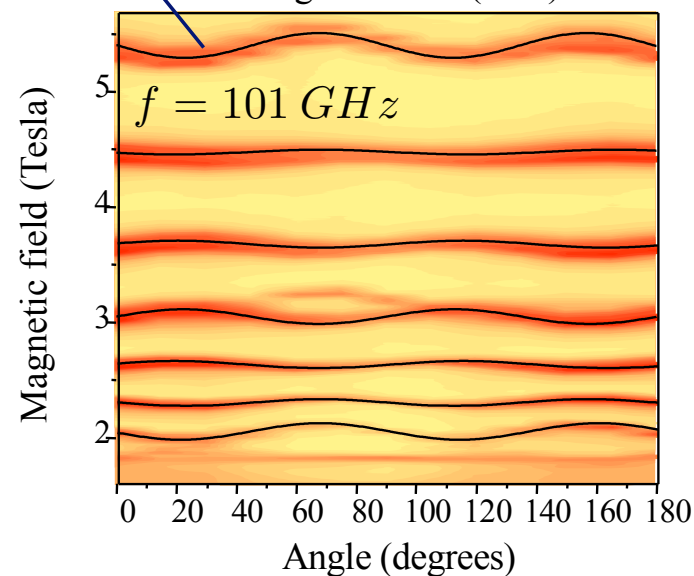
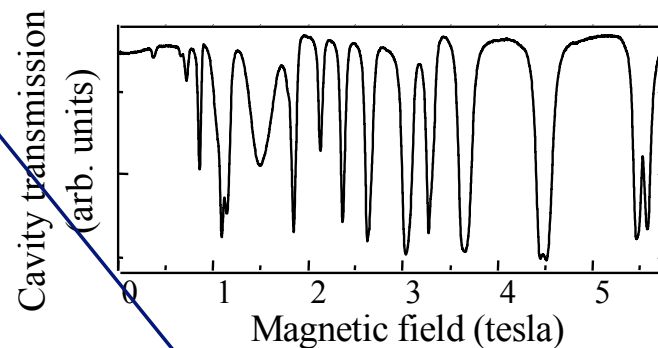
$$D_U = -0.577 \text{ cm}^{-1}$$

$$B_4^0 = -0.00012 \text{ cm}^{-1}$$

$$B_4^4 = -0.0004 \text{ cm}^{-1}$$

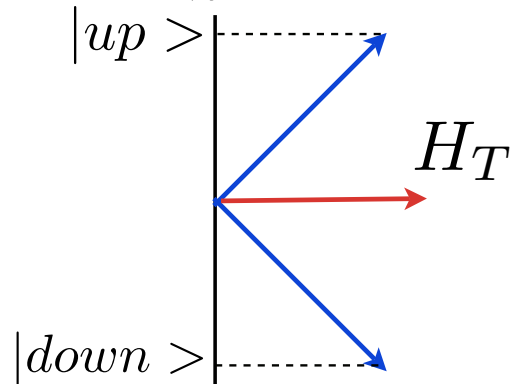
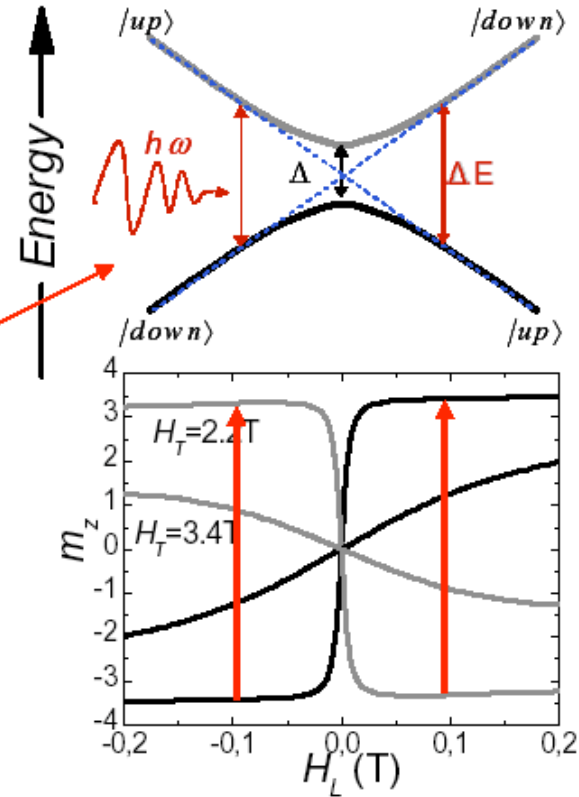
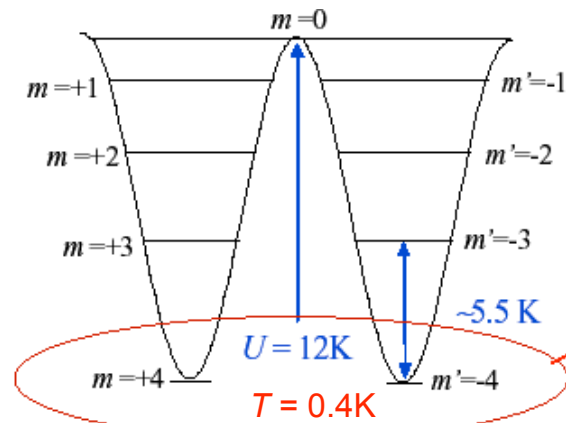
$$g_z = 2.30$$

$$g_x = g_y = 2.23$$



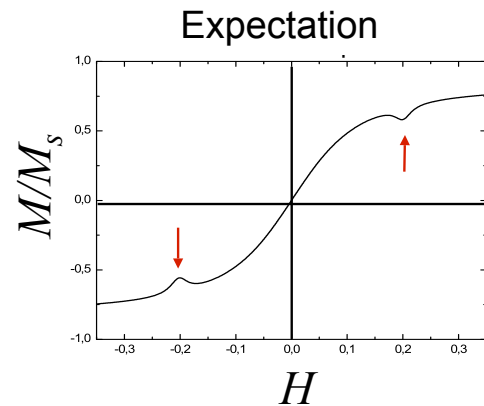
Multiple but narrow peaks – “molecular environments” with slightly different D values

Experiment

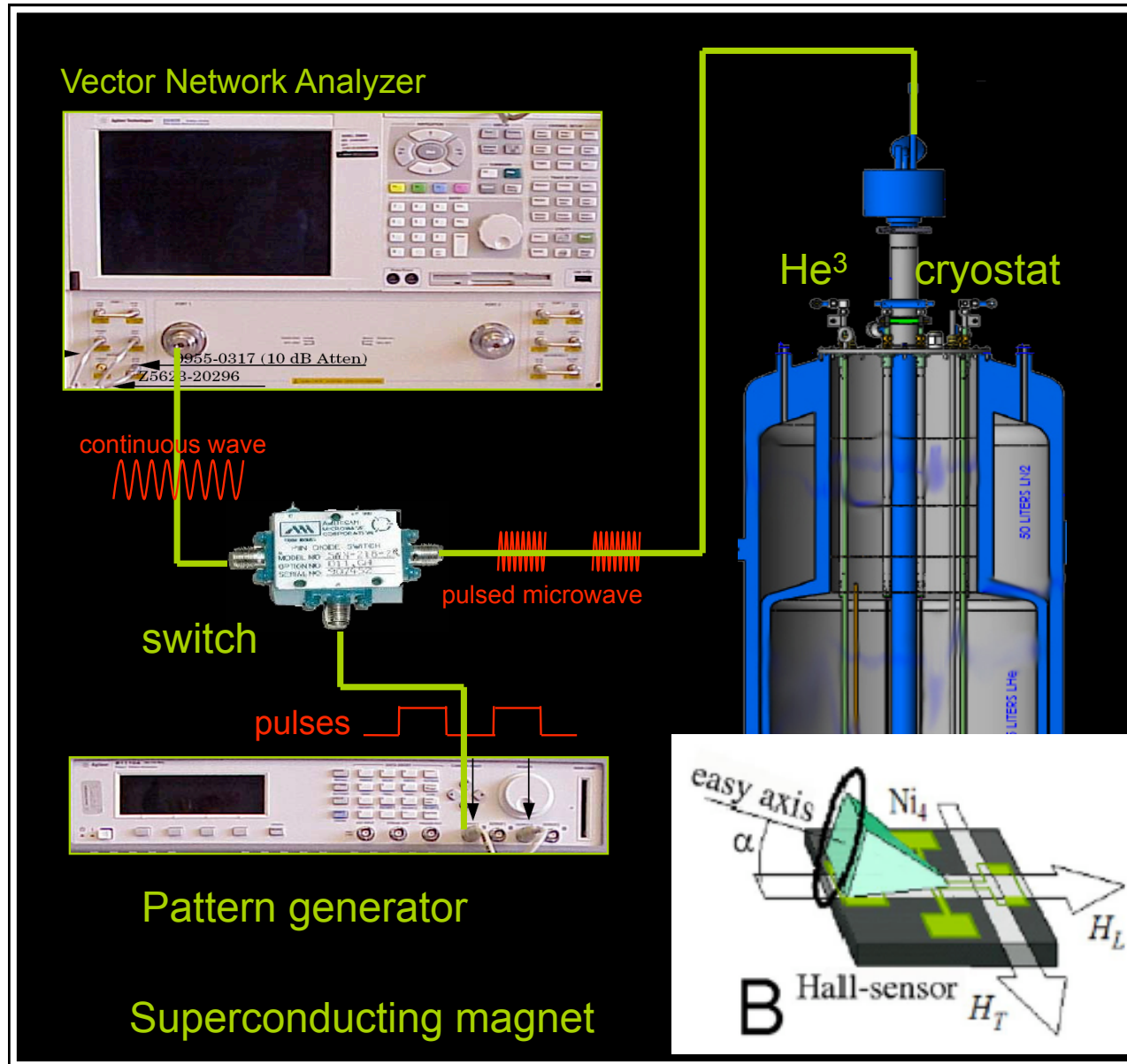


$$|S\rangle = \frac{1}{\sqrt{2}} (|up\rangle + |down\rangle)$$

$$|A\rangle = \frac{1}{\sqrt{2}} (|up\rangle - |down\rangle)$$

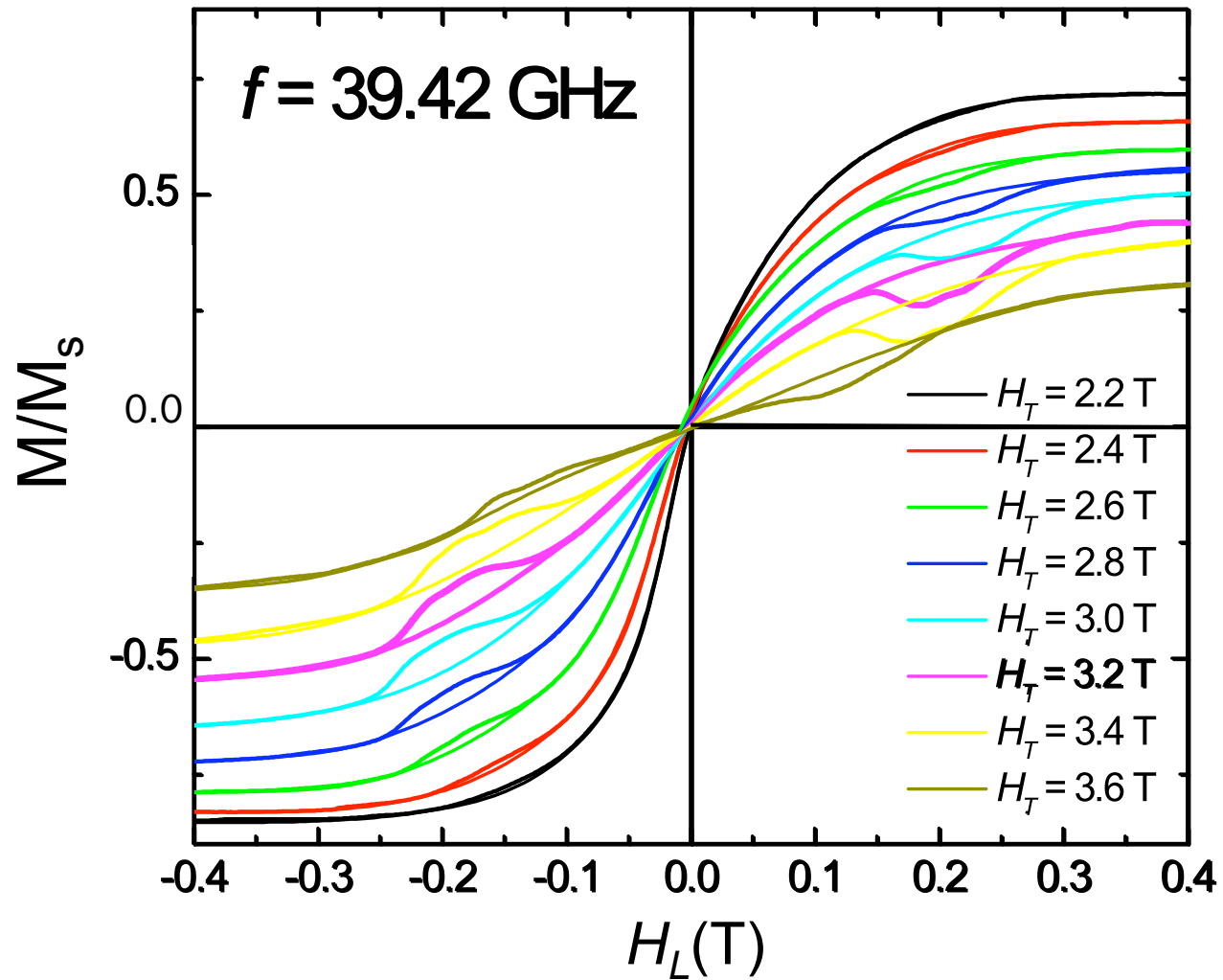


Experimental Setup



Results: Photon Induced Transitions between Superposition States

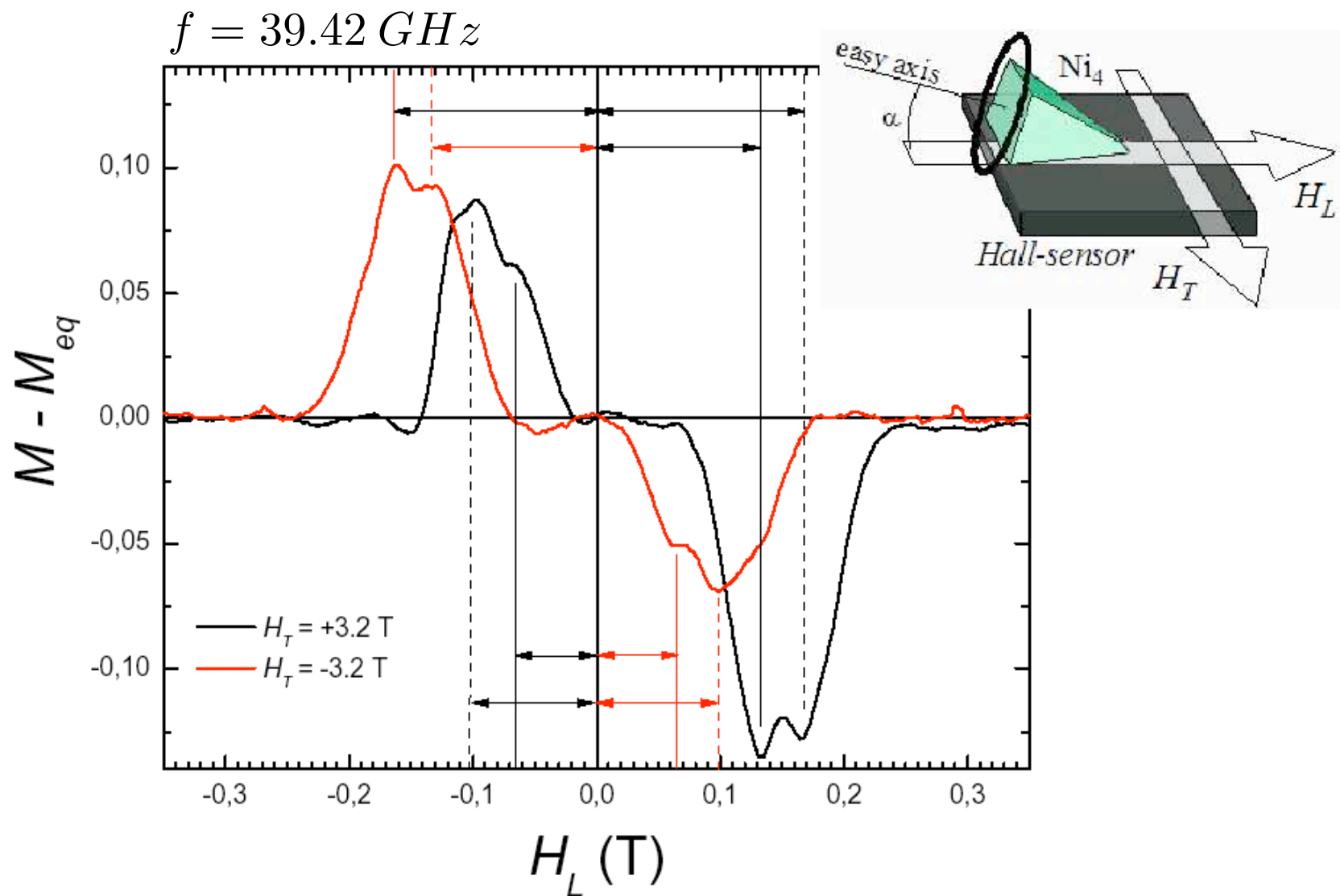
Magnetization with microwaves



$T = 0.45 \text{ K}$

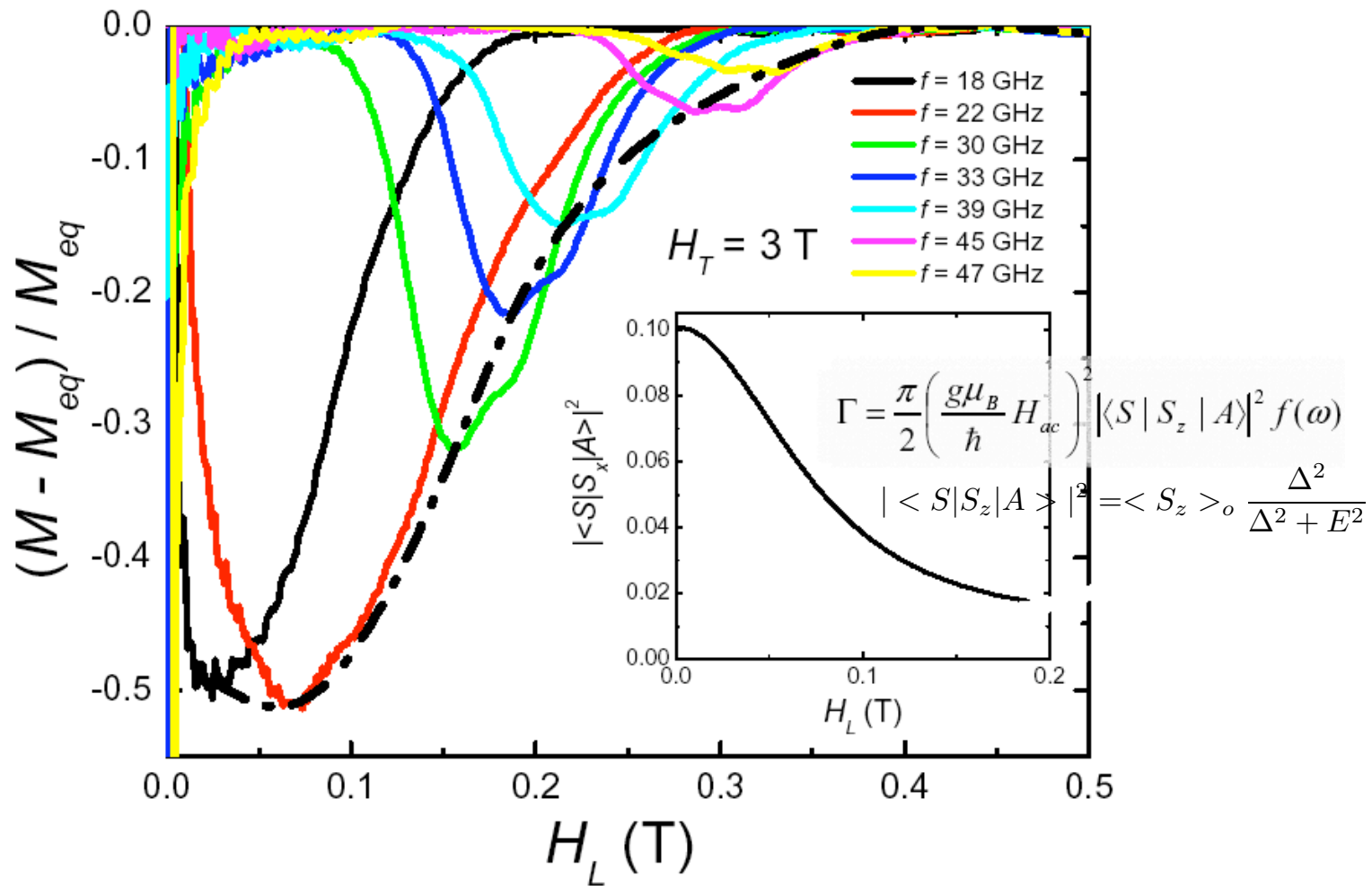
$\Delta T < 0.01 \text{ K}$ in the peaks

Results: Photon Induced Transitions between Superposition States

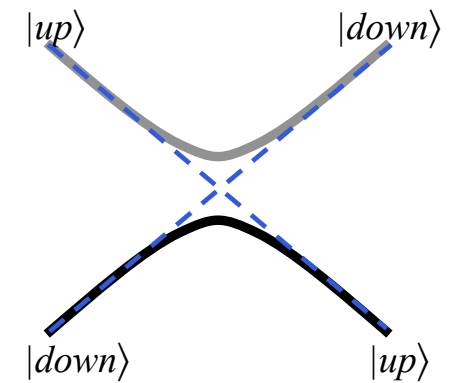
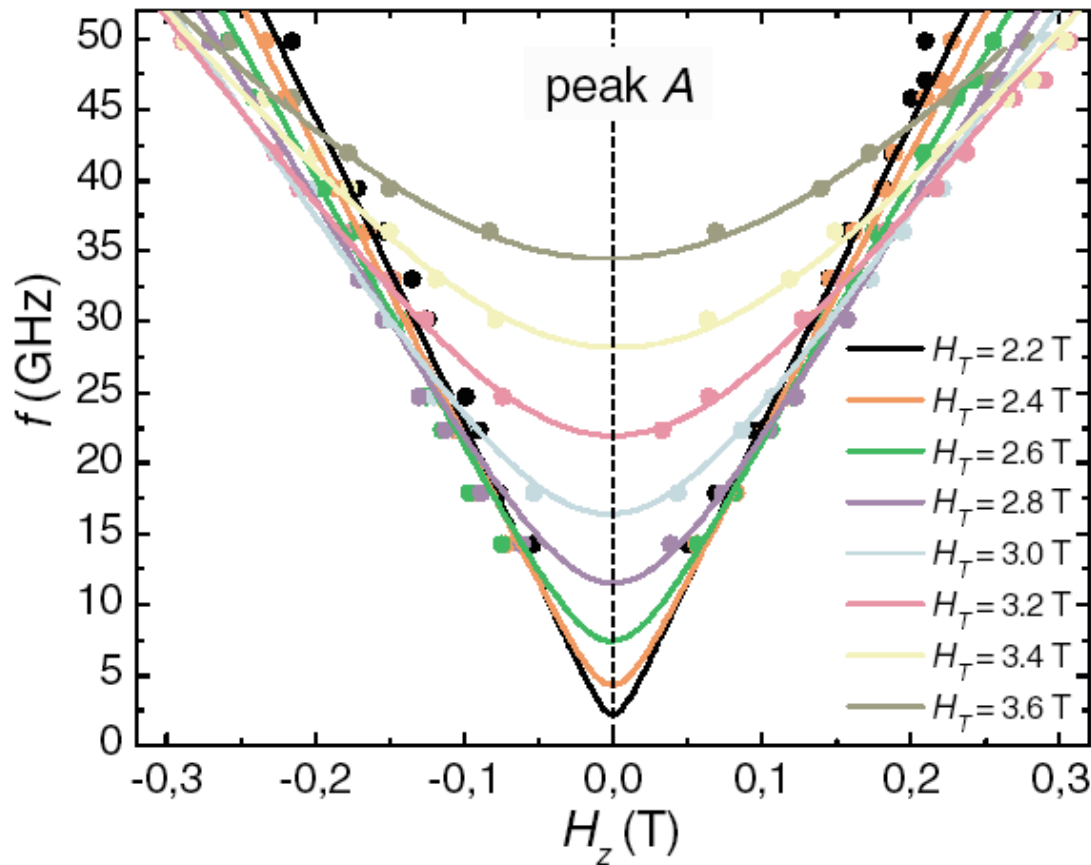


Results: Photon Induced Transitions between Superposition States

Amplitude vs. frequency

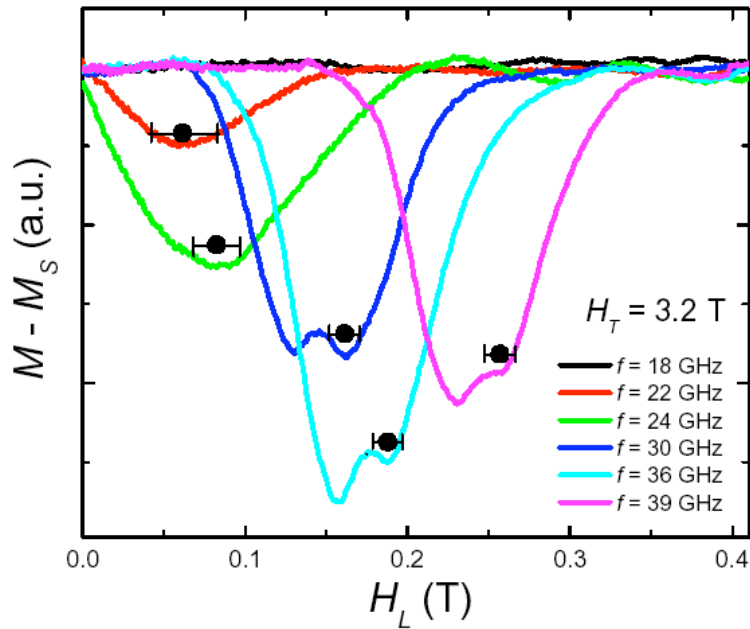


Results: Photon Induced Transitions between Superposition States

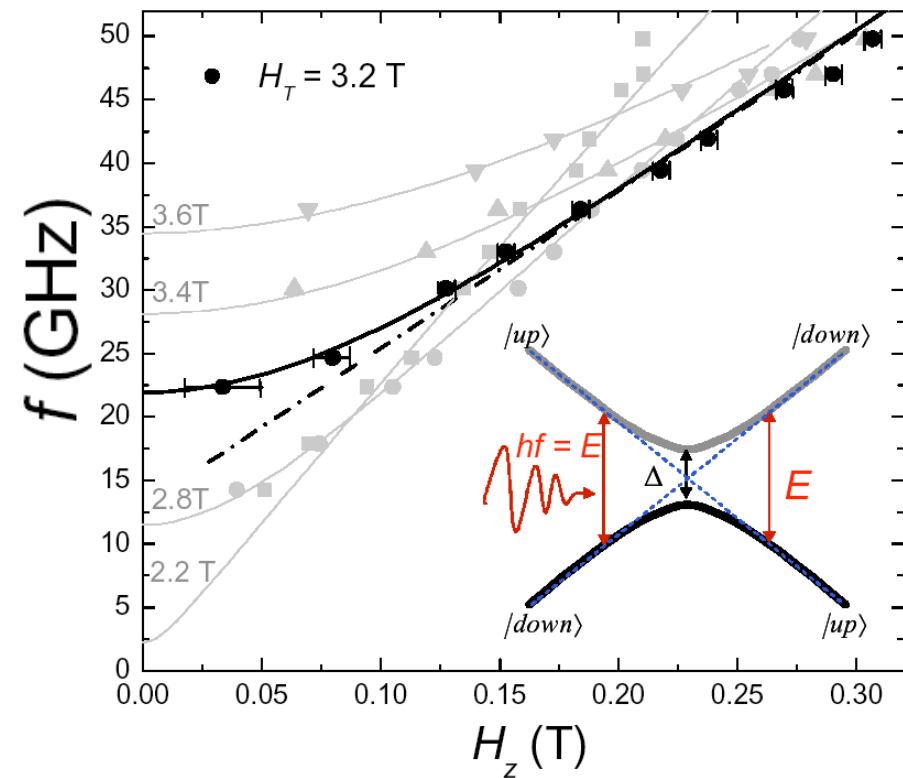


Level Repulsion: Observation of quantum superposition of high spin states with opposite magnetization

Results: Photon Induced Transitions between Superposition States



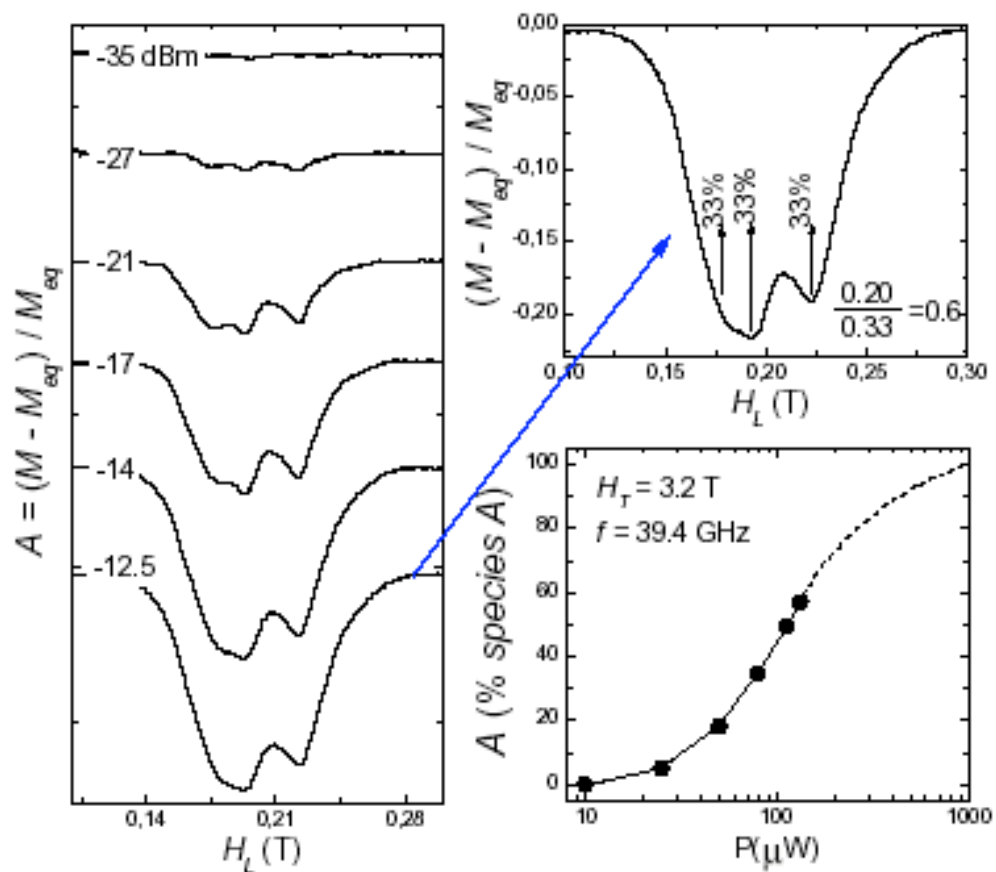
Curvature



Approach to saturation and Ni₄ 'micro-environments'

As a function of mw power – cw radiation

$$H_T = 3.2 \text{ T} \quad f = 39.4 \text{ GHz} \quad P_{\text{loss-in-coax}} = 15 \text{ dB}$$

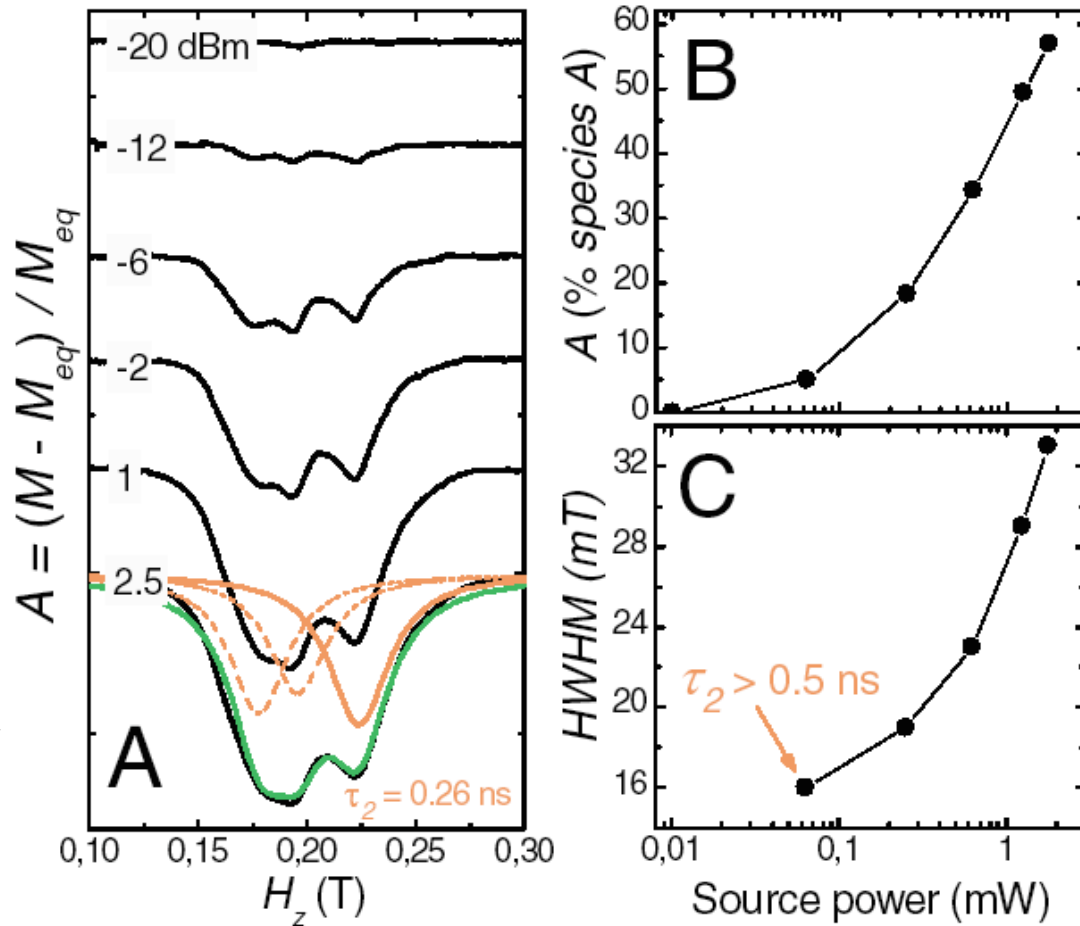


Results: Transverse relaxation rate (τ_2) – decoherence (τ_ϕ)

Decoherence time lower bound

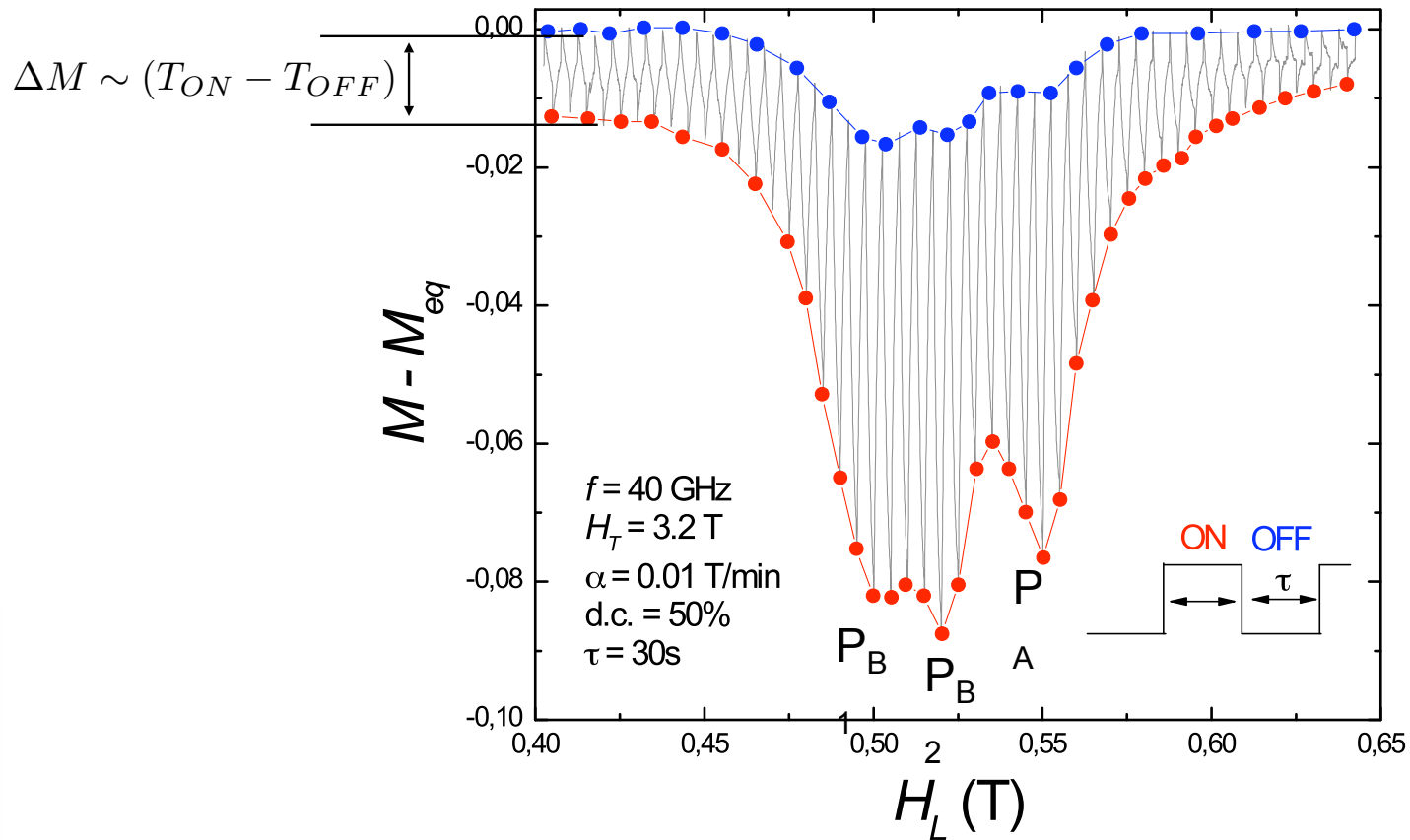
$H_T = 3.2 \text{ T}$ $f = 39.4 \text{ GHz}$

$$f(\omega) = \frac{1}{\pi} \frac{\tau_2}{1 + (\omega - \omega_0)^2 \tau_2^2}$$



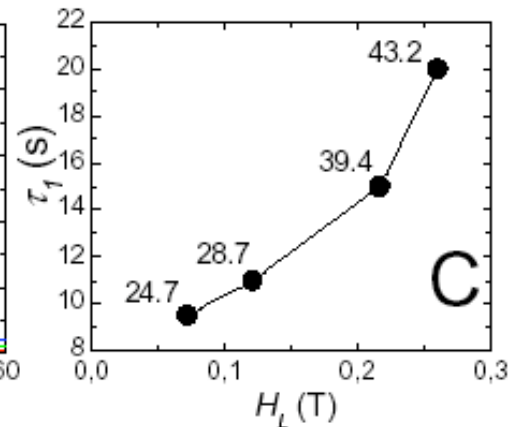
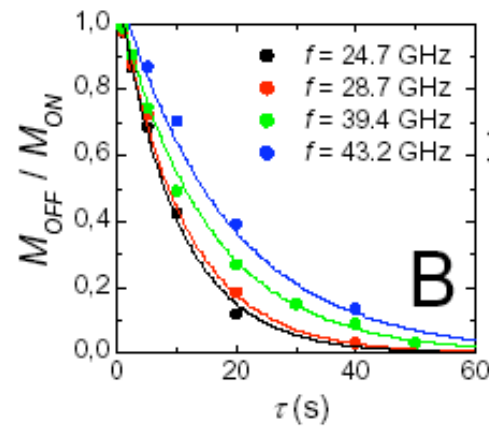
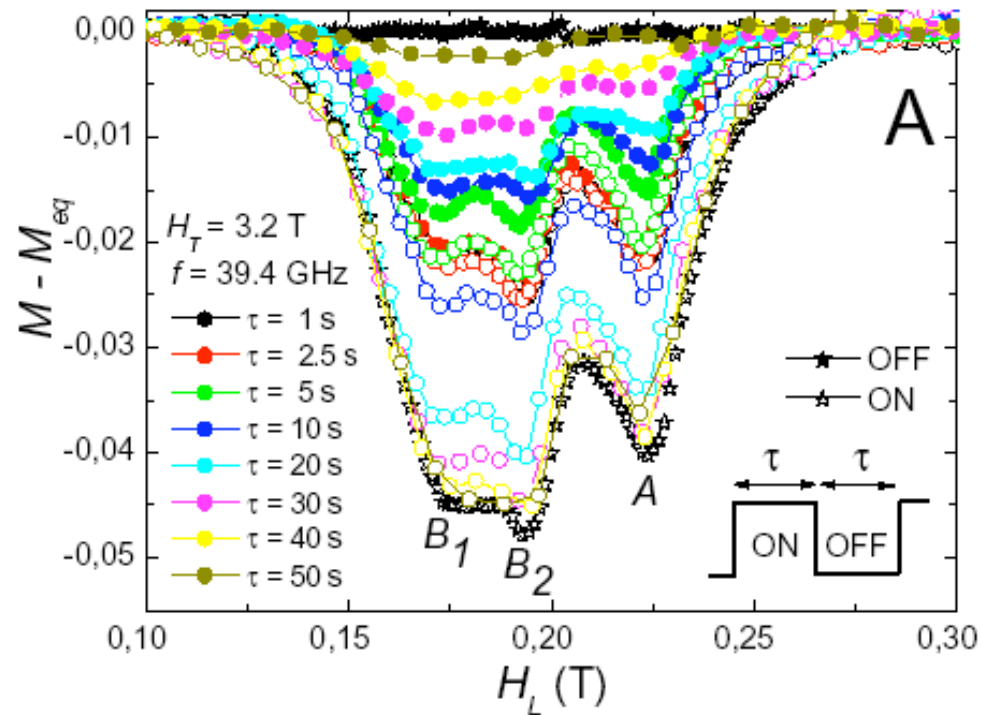
Results: Longitudinal relaxation rate

Pulsed microwave radiation experiments



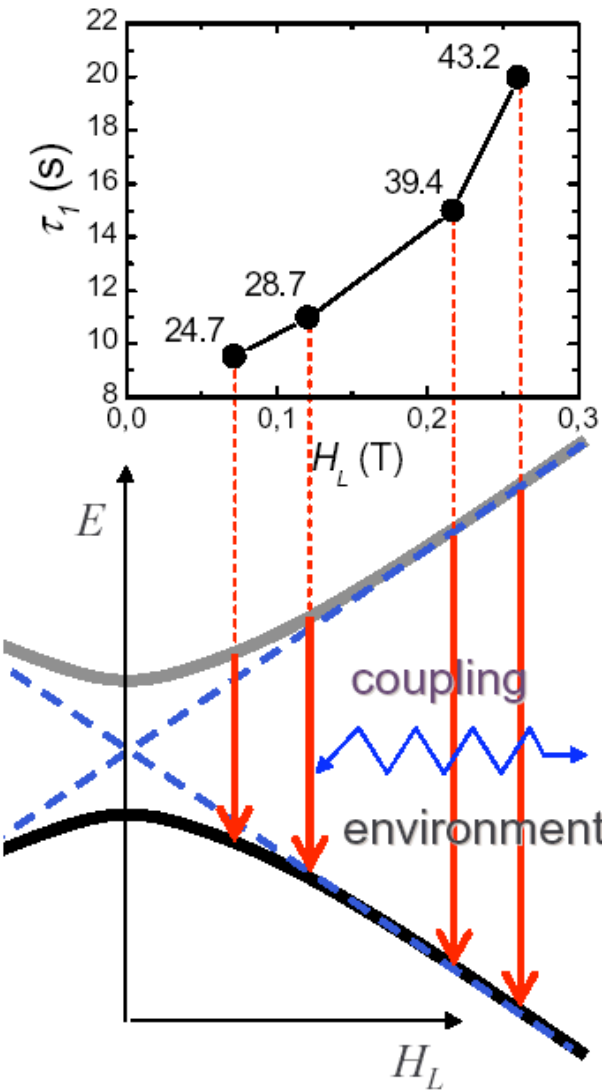
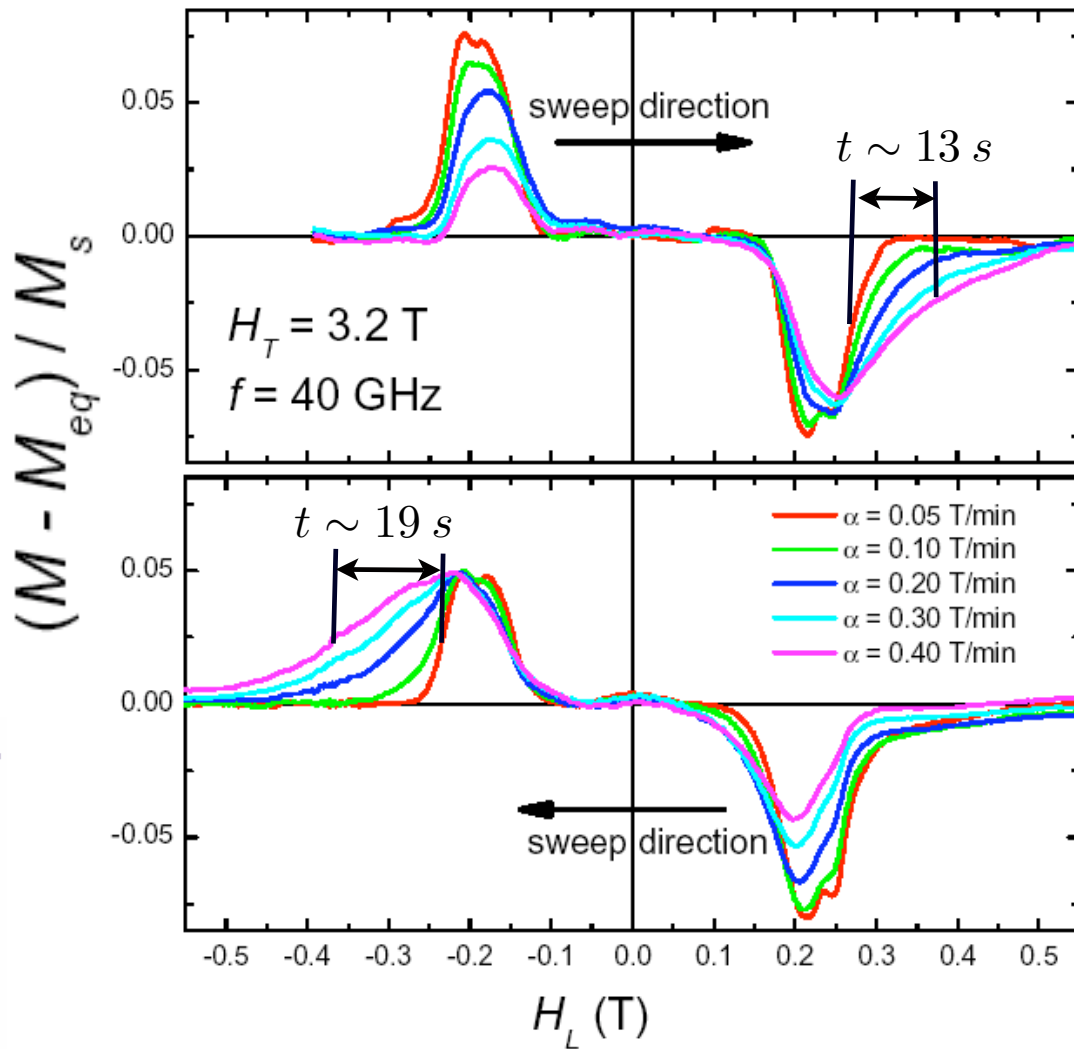
Results: Longitudinal relaxation rate

Pulsed microwave radiation experiments



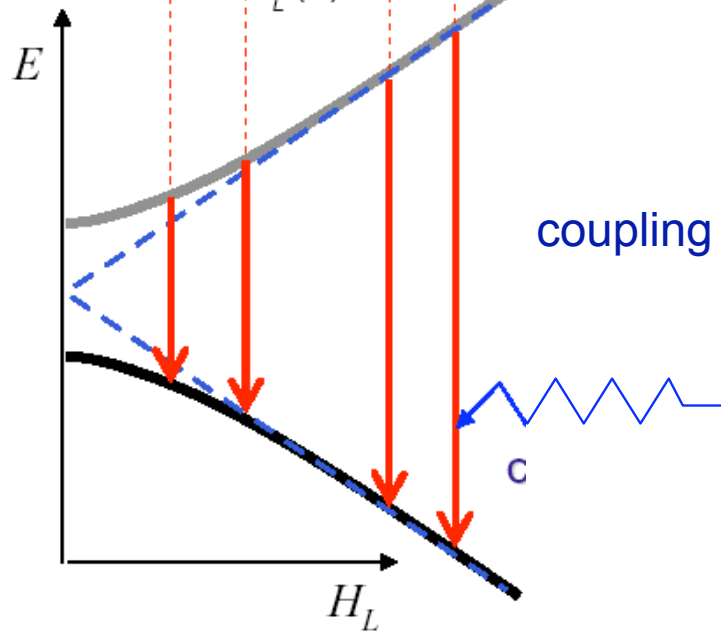
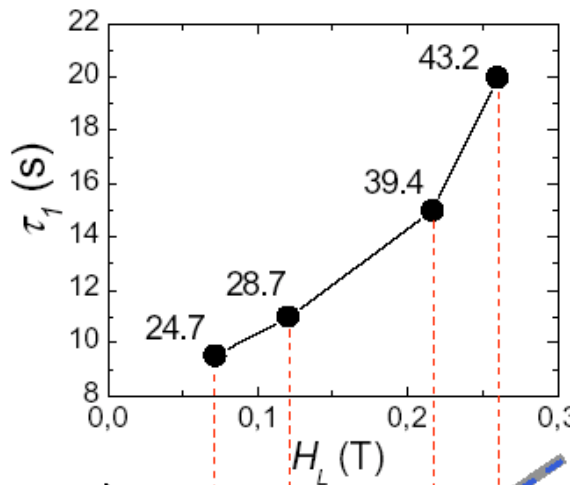
Longitudinal relaxation effects in cw experiments

Energy relaxation time increases with longitudinal field and frequency!



Spin-Phonon Relaxation

Pulsed radiation experiments



Relaxation rate:

$$\tau_1^{-1} = \Gamma_1 = \frac{S^2 \Delta^2 \omega^3}{12\pi \hbar^2 \rho c_t^5} \coth\left(\frac{\hbar\omega}{2kT}\right)$$

Chudnovsky, PRL 2004

$$c_t = 10^3 \text{ m/s}, \quad f = \Delta/h = 20 \text{ GHz}$$

$$\tau_1 = 10^{-3} \text{ sec}$$

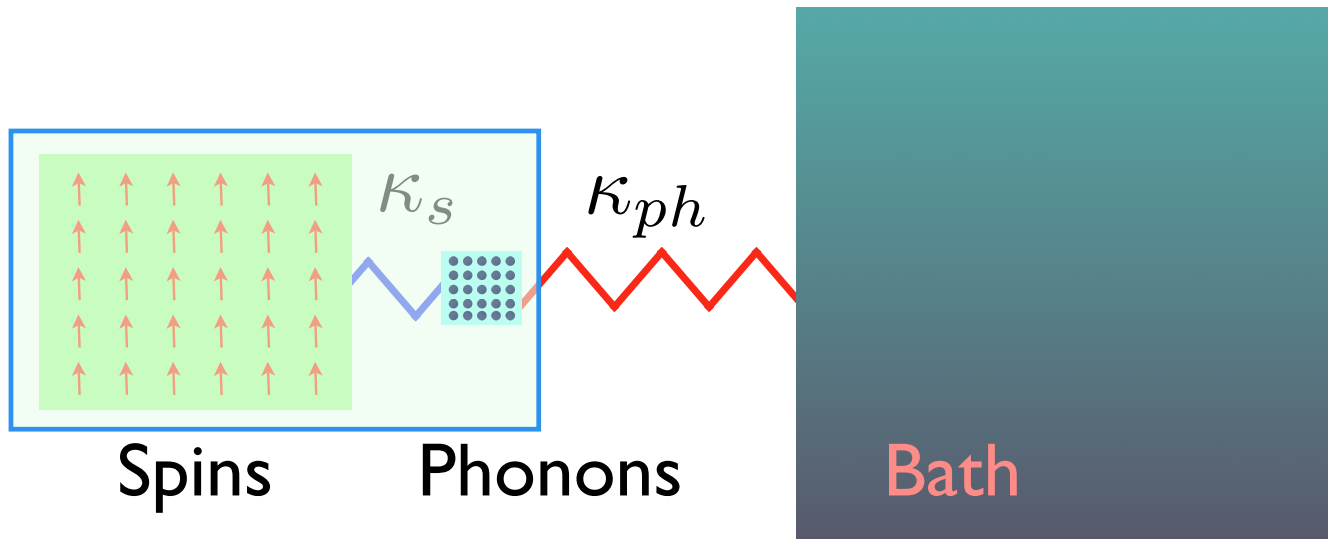
Upper limit on the relaxation time!

Phonon-laser effect:

$$\Gamma_L \sim \omega^{-3}$$

Chudnovsky and Garanin, PRL 2004

Spin-Phonon Bottleneck

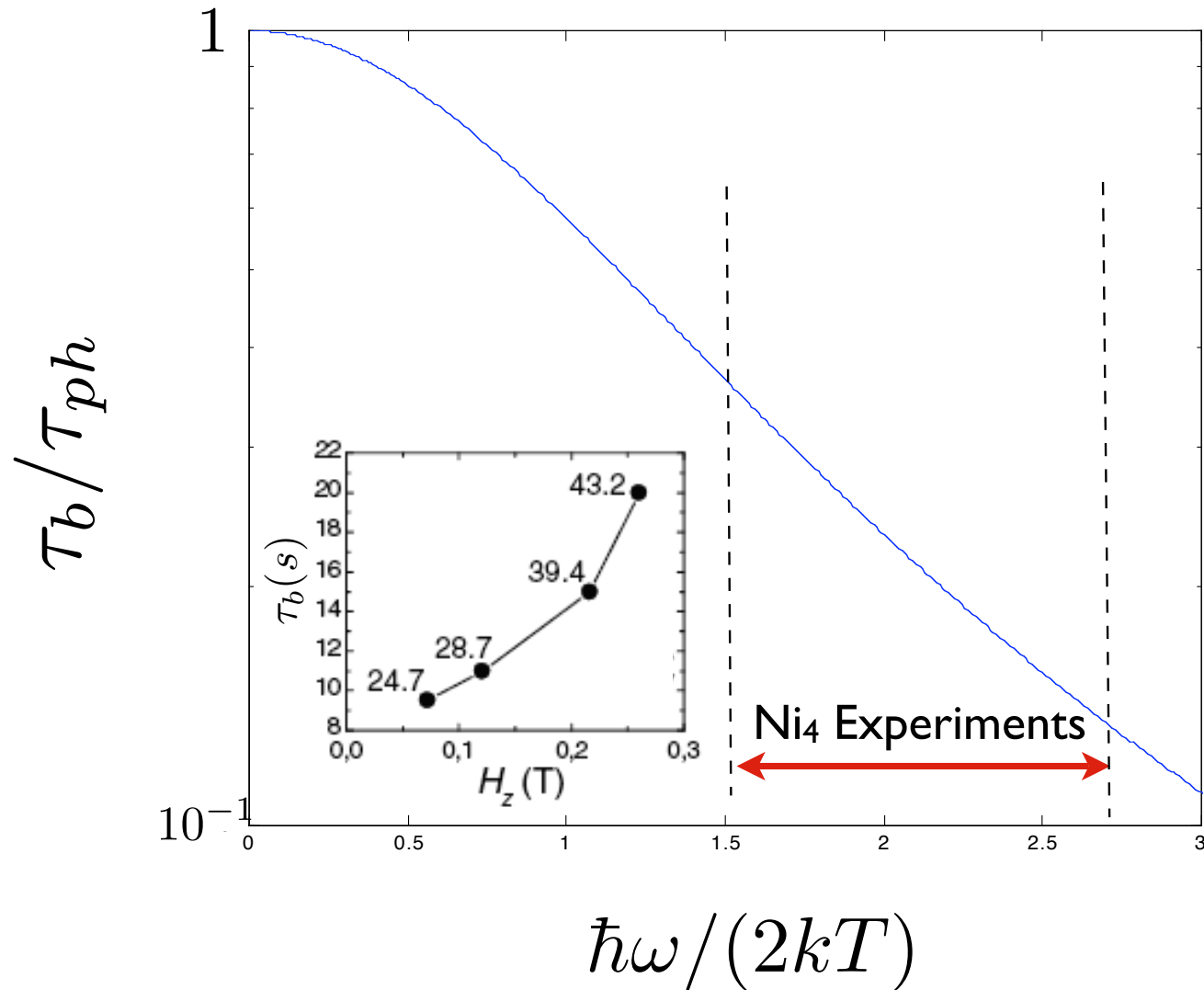


- Bottleneck arises because: $\kappa_s \gg \kappa_{ph}$
 - Small amount of heat is transferred from the spin to resonant phonons
 - Resonant phonons are heated rapidly, because of their small heat capacity or density of states.
 - T_{phonons} rapidly approaches T_{spins} $\tau \sim \frac{C_{\text{phonons}}}{C_{\text{spins}}} \tau_1$
 - Spins and phonons are strongly coupled in terms of relaxation
 - Combined system relaxes slowly:

$$\tau_b = \tau_{ph} (C_{\text{Spins}} / C_{\text{Phonons}})$$

Effective Relaxation Time versus Frequency

Bottleneck Physics (Classical Thermodynamic Picture)



Summary (Ni₄)

- Observation of energy splittings between low-lying superpositions of high spin-states.
 - Direct measurement of the magnetization combined with microwave spectroscopy
- Lower bound for the decoherence time $\tau_\phi > 0.5$ ns
 - Similar to that observed in the Mn₄-dimer through EPR measurements a system with strong intermolecular exchange interactions
- Determination of the longitudinal relaxation times $\tau \sim 10$ -20 s
 - Characterized τ as a function of longitudinal field and frequency